AN ASSESSMENT OF ATLANTIC BIGEYE TUNA FOR 2015

Michael J. Schirripa[1]

SUMMARY

An initial assessment of the Atlantic bigeye tuna stock was conducted in advance of the full 2015 SCRS Bigeye Tuna Stock Assessment meeting. The evolution of the fishery from a predominately longline catch to one of increasing purse seine catch violates important assumptions of stock-production models, therefore an integrated model approach may be more appropriate. The fully integrated stock assessment framework Stock Synthesis was used to construct a three area, four season model that consisted of fifteen fleets, representing the three major gear types (longline, purse seine, and baitboat) in time and space. Three candidate model configurations are presented for further consideration, with one proposed as a base model. Examination of the catch-at-age estimates showed that the percent of landings accounted for by the purse seine gear has steadily increased over time. As such, landings of age 0 and age 1 fish are becoming a higher proportion of the total catch, which has led to a down turn in the yield-per-recruit. Given the nature of the purse seine gear, the fishery and its CPUE may be exhibiting hyper-stability which may be biasing model results. Model results indicated that spawning stock biomass and recruitment have been steadily declining. The CPUE data used to fit the model tend to indicate a less productive stock while the information within the length and size-at-age data indicate a higher productivity.

RÉSUMÉ

Une évaluation initiale du stock de thon obèse de l'Atlantique a été réalisée avant la réunion SCRS d'évaluation complète du stock de thon obèse de 2015. L'évolution de la pêcherie, où les prises palangrières dominaient pour faire place ensuite à des prises à la senne de plus en plus fortes, enfreint d'importants postulats de modèles de stock-production ; c'est pourquoi une approche de modèle intégré pourrait s'avérer plus appropriée. Le cadre d'évaluation des stocks entièrement intégré Stock synthèse a été utilisé pour élaborer un modèle à trois zones et à quatre saisons qui était composé de 15 flottilles, représentant les trois principaux types d'engin (palangre, senne et canne) dans le temps et dans l'espace. Trois possibles configurations du modèle sont présentées afin d'être examinées plus avant, l'une étant proposée comme cas de base du modèle. L'examen des estimations de la prise par âge a montré que le pourcentage des débarquements des captures réalisées à la senne a régulièrement augmenté dans le temps. Ainsi, les débarquements de poissons d'âge 0 et 1 représentent une proportion plus importante de la prise totale, ce qui a entraîné une baisse de la production par recrue. Compte tenu de la nature de l'engin de senne, la pêcherie et sa CPUE pourraient faire apparaître une hyper stabilité, ce qui pourrait fausser les résultats du modèle. Les résultats du modèle ont indiqué que la biomasse du stock reproducteur et le recrutement ont régulièrement diminué. Les données de CPUE utilisées pour ajuster le modèle tendent à indiquer que le stock est moins productif tandis que l'information contenue dans les données de taille et de taille par âge indique une plus grande productivité.

RESUMEN

*Las oscilaciones atmosféricas afectan directamente a muchas especies migradoras, reflejado en un cambio directo en su abundancia, reclutamiento o condición física. Este estudio tiene como principal objetivo elucidar posibles efectos de las oscilaciones climáticas (estandarizada por el índice NAO) sobre la condición física de la melva (*Auxis rochei*). Para ello se analizó el índice de condición de 2.154 ejemplares capturados mediante diferentes artes de pesca por pesquerías comerciales a lo largo de la costa Mediterránea española durante los periodos comprendidos entre 1983-1984 y 2003-2014. Las capturas tuvieron lugar durante el movimiento migratorio que esta especie realiza hacia las áreas de puesta situadas en el Mediterráneo occidental. La condición física se probó en relación con las oscilaciones atmosféricas teniendo en cuenta la*

[1] NOAA Fisheries, Southeast Fisheries Center, Sustainable Fisheries Division, 75 Virginia Beach Drive, Miami, FL, 33149-1099, USA; Email: Michael.Schirripa@noaa.gov

edad y ratio de sexos. Se obtuvieron diferencias significativas entre el índice de condición para los individuos de clase de edad 2+ y los índices NAO_w y NAO_{ant}. En los años con un índice NAO positivo se observó una mejor condición física en los ejemplares estudiados. Esto podría deberse a que las condiciones ambientales durante los años de NAO en fase positiva facilitarían la migración. No obstante, se recomienda continuar con el seguimiento de las poblaciones para poder elucidar los efectos climáticos sobre la condición física de esta especie migratoria.

KEYWORDS

Bigeye tuna, Stock assessment, Fishery Management, Population dynamics, Yield/recruit

1. Description of the Fishery

Historically the Atlantic bigeye tuna stock has been exploited by three major gear types (longline, baitboat and purse seine fisheries) and by many countries throughout its range of distribution and ICCAT has detailed data on the fishery for this stock since the 1950s. Scientific sampling at landing ports for purse seine vessels of the EU and associated fleets have been conducted since 1980 to estimate bigeye tuna catches (**Figure 1**). The size of fish caught varies among fisheries: medium to large for the longline fishery, small to large for the directed baitboat fishery, and small for other baitboat and for purse seine fisheries.

The major baitboat fisheries are located in Ghana, Senegal, the Canary Islands, Madeira and the Azores. The tropical purse seine fleets operate in the Gulf of Guinea in the East Atlantic and off Venezuela in the West Atlantic. In the eastern Atlantic, these fleets are comprised of vessels flying flags of Ghana, EU-France, EU-Spain and others which are mostly managed by EU companies. In the western Atlantic the Venezuelan fleet dominates the purse seine catch of bigeye tuna. While bigeye tuna is now a primary target species for most of the longline and some baitboat fisheries, this species has always been of secondary importance for the other surface fisheries. In the surface fishery, unlike yellowfin tuna, bigeye tuna are mostly caught while fishing on floating objects such as logs or man-made fish aggregating devices (FADs). During 2010-2012, landings in weight of bigeye tuna caught by the longline fleets represent 53%, purse seine fleets represent 32% and baitboat fleets represent 14% of the total bigeye tuna catch (**Figure 2**).

One of the advantages of using Stock Synthesis (SS) is the incorporation of spatial structure so that the movements among regions can be estimated. In this study, we took a first step by taking simple and large 3 regions (north of 25N, between 25N and 15S, and south of 15S) separating out tropical and temperate waters as shown in **Figure 3**. Although finer spatial structure might be adopted, the limited amount of tagging data, from which information on migration is estimated, makes difficult to estimate migration. These regions can be modified and more detailed and a more suitable stratification might be adopted in the future. Due to non-occurrence of bigeye in the higher latitudes, north of 50ºN or south of 50ºS were excluded from the analysis.

It is difficult to discriminate a fishing effort for free schools (composed of large bigeye tuna) for FAD fishing (targeting skipjack, yellowfin, and bigeye tuna) in the East Atlantic because the fishing strategies can change from one year to the next and in addition, the sea time devoted to activities on FADs and the assistance provided by supply vessels are difficult to quantify. The Committee recognizes that the use of data series on the yearly progression of the sale prices of tropical species by commercial category enables identification of the years when skipjack is most targeted by the purse seiners (which seems to be the case in the past few years, **Figure 4**). Nominal purse seine effort, expressed in terms of carrying capacity, has decreased regularly since the mid-1990s up to 2006. However, after this date, several European Union purse seiners have transferred their effort to the East Atlantic, due to piracy in the Indian Ocean, and a fleet of new purse seiners have started operating from Tema (Ghana), whose catches are probably underestimated. All this has contributed to the growth in carrying capacity of the purse seiners, which is gradually nearing the level observed in the early 1990s (**Figure 4**). The number of purse seiners follows this trend but seems to have remained steady since 2010; the nominal effort of baitboats has remained stable for over 20 years.

The mean size of bigeye tune was relatively stable for each of the major gear types up until about the year 2000. Starting around 2000 the mean size of longline caught fish from the core area began a steady increase from approximately 120 cm to approximately 140 cm (**Figure 5**). During this same time mean size of fish caught by the northern bait boat remained stable at approximately 100 cm. The two purse seine fisheries currently still in operation (free school and FAD) showed different trends. The free school fishery mean size has been much less stable, varying between 60 to80 cm, while the FAD caught fish mean size remained stable but with a sharp shift in 1997 to smaller fish (< 60 cm). The mean size of all five fisheries examined all showed an increase in mean size in the most recent years. This could be due to a shift in effort to larger fish or, perhaps more likely, to a decrease in smaller fish, presumably due to declining recruitment.

2. Observational Data

2.1 Growth

Growth was modeled by fitting a growth curve within the model framework. The model was provided the estimated mean size at age from 10 different studies/growth curves on Atlantic bigeye tuna as described in Brown (2005 Col. Vol. Sci. Pap. ICCAT, 57(2): 94-114 (2005)). While using size-at-age from estimated growth equations is not the ideal practice, it does offer the ability to incorporate between-study error into the estimates of growth. Furthermore, since some studies used hard part analysis, others length frequency, and still others tagging information, the data sets were not compatible with each other so as to use them as actual data within the assessment model fitting process. In this method all three growth parameters (L_1, L_2, and k) were freely estimated. Variation is size-at-length was described as a function of length-at-age using a coefficient of variation 10.0% for all ages.

A separate growth curve was considered for comparison purposes that was designed to mimic the two-stanza growth reported by Fonteneau (2013; IOTC–2013–SC16–INF06). This work modified the growth curve used in the IOTC assessment from Everson et al. (2015) for assigning fish at length 50 cm to age_2, and suggested that 50 cm fish are in fact mostly age_1. The equation to describe the growth function from this paper was not available, so one had to be built. The parameters of the equation were approximated by fitting an SS "growth only" model to the Fonteneau curve values as observed data, and as the only observed data, and by (1) allowing for four *k*-deviates in the growth curve for ages 1, 2, 3, and 4; (2) fixing the size-at-age_1 and the size-at-age_10 parameters to those predicted by the Fonteneau curve (51.2 cm and 157.0 cm) and allowing *k* and the four *k*-deviates to be estimated. This produced a curve that was nearly identical to that described in the Fonteneau paper and captured the major conclusion of the work. The Indian Ocean growth curve L-infinity was considerably smaller than any of the values or observations from the Atlantic (**Figure 6**). One reason for this may be that bigeye tuna from the Indian Ocean do not have access to the higher latitudes that the Atlantic fish do. Annual migrations to higher latitudes in the Atlantic are generally associated with feeding on prey of higher fat and lipid content than those found in the tropics. This higher caloric food could account for fish growing larger in Atlantic than in the Indian Ocean. For these reasons, the Indian Ocean growth curve was not considered for assessment purposes.

It should be noted that the most influential differences between the ATL-ICCAT and the MOD-IOTC model are in the values at young ages, but rather in their respective $L\infty$. The ATL-ICCAT model has an $L\infty$ of ~210 cm while the MOD –IOTC was closer to ~160 cm. Brown (2005) reported the range of maximum size from all the Atlantic growth models considered in that work and found a range of 155-190 cm. Furthermore, recent work by Minte-Vera et al (2015) estimated four possible growth models for bigeye tuna in the eastern Pacific Ocean and obtained values of 199, 236, 288, and 212 cm. Given these observations, the $L\infty$ of ~210 cm may be a more plausible value.

2.2 Indices of Abundance

Indices of abundance representing eight of the fifteen fleets where available: a purse seine index, a bait boat index, and six longline indices. The purse seine CPUE was made available after the data preparatory meeting. Note that all of the CPUE's indices are shown on a log scale to better show the year-to-year contrasts. This index of abundance was assigned to the purse seine fishery on FADs (fleet 4, Area 2, **Figure 7, top**). This fleet captures mostly age_0 and age_1 fish, thus this CPUE could be quite influential on the estimates of annual recruitment.

There is an apparent downward trend to the CPUE over the time series. It should also be noted that the catchability of the FAD purse seine fleet is thought to perhaps be increasing over time. If so, the downward trend would be dampened by this fact. The trend ends with a sharp decrease in the CPUE in the last year (2014).

The bait boat indices represented the fleet fishing Azores Inlands (fleet 9, Area 1, **Figure 7, bottom**). During the data preparatory meeting it was shown there was a negative correlation between the summer Atlantic Multidecadal Oscillation (AMO) and the CPUE from the Northern Islands bait boat fishery (**Figure 8, top**). The AMO is the 10-year, area weighted, running average of the SST of the area between 0-60 degrees latitude. The hypothesis behind this correlation was that the annual migration of bigeye from the spawning area (Area 2 in the model) to their northern feeding ground (Area 1 in the model) could be indexed by the AMO. The direct mechanism behind this connection could range from habitat preference to food availability, or both (or neither). However, it has been recognized for at least twenty years that movement and migratory patterns of Atlantic bigeye tuna can be influenced by oceanographic conditions:

"The strong inter-annual variability observed in the Portuguese and Canary Islands baitboat catches is most likely die to the variations in the local hydrological conditions" (SCRS 94-95).

It seems plausible that the drop in approximately 1995, which corresponds with the switching of the AMO at that same time, may have some influence not on stock biomass, but rather on the rate of northward movement to Azores Islands. This is especially supported by the strong match between the AMO and the changing CPUE in 1987, 1990, and again in 1995. The regression of the CPUE on the summer AMO (the mean of July, August, and September) shows that the AMO explains 46% of the variation in the CPUE (**Figure 8, bottom**).

The Japanese longline CPUE data provided area-specific indices for all three areas (**Figure 9**). Areas 1 and 2 showed increasing trends at the beginning of the times series, often thought to be period of learning how to effectively catch bigeye. Then, around 1980, both areas show declining trends. In 2010 however, Area 1 showed a sharp decline (similar to the purse seine index previously discussed), while at the same time Area 2 showed an uptick. As discussed previously, it's possible that these contrasting patterns are at least partially reflective of time varying movement rates between Areas 1 and 2, and not necessarily entirely attributable to changes in stock biomass.

The United States longline CPUE was used to index larger fish in Area 1 (**Figure 10**, top). The Chinese -Taipei CPUE was split into two indices by the CPC based on the source of the (logbooks versus landings statistics) (**Figure 10**, middle). To accommodate this break in the CPUE time series two different catchabilities were estimated, one for each time period. A similar approach was used for the Uruguayan CPUE as it was provided in a two part series as well (**Figure 10**, bottom) and was used to index the larger fish in Area 1 in the south.

The indices of abundance were not in full agreement with each other. Overall, there was a long term declining trend consistent with all indices but differences in the most recent years were evident. The apparent difference could be possibly be explained by different selectivities (which are accounted for in the assessment model) and/or differences between the area they represent. Differences could also be due to inconsistent migration rates or juvenile survival between areas. Without long term, informative tagging data that covers movements between all the areas it is not possible to test any hypotheses regarding this possibility. However, changes in length compositions indicated that a change in some selectivities was evident (see below).

2.3 Length Compositions

Length composition was provided by the ICCAT secretariat. Unlike with the VPA analysis, estimates of catch-at-size (CAS) were not used in the SS platform. Rather, the length observations were used directly with no expansion factor applied. Year, quarter combinations with less than 50 observations were deleted from the data. Data from the purse seine fleets 1, 2, and 4 are shown in **Figure 11**. The purse seine fleet catches mostly small fish, age_0 and age_1. The bimodal distributions of each of the fleets are due to the boats fishing either schools of small fish, or having larger schools pointed out them to exploit. In this way the mean size (denoted by the red lines) can increase either by the fleet catching more of the larger fish or fewer smaller fish.

The true baitboat fleets catch medium sized fish, approximately 100 cm, or about age 3 (**Figure 12**). However, some in some cases, such as the Ghana, the baitboat lengths were combined with the purse seine lengths.

The longline fleets catch the largest bigeye (**Figure 13**). There was an apparent shift in length compositions for "other longline fleets in Area 2 (fleet 14) in 2006. The data indicates that smaller fish were no longer being caught and that larger fish were now being harvested. While this pattern could be indicator of stock structure, it is much more likely explained by a change in fishing and/or gear methods. Curious, and quite possibility coincidental, is that this change in length composition happened at the same time there was a shift in the length comps of purse seine free school fleet (fleet 3, also in Area 2).

2.4 Movement

The between-area movement of bigeye tuna was modelled to reflect the assumption that spawning takes place in the winter (season 1; Jan, Feb, Mar), and mostly in Area 2. An annual migration of at least part of the spawning stock begins in the spring (season 2; April, May, June) from the spawning area, northward to feeding areas (Area 1). In season 4 (Oct, Nov, Dec) fish moved back to Area 2. During the Data Preparatory meeting the tagging data was shown not to be informative for movement (**Figure 14**), rather it was CPUE and length compositional data that accounted for the parameter values. This is further evidenced by the fact that very many of the fish tagged in Area 2 were also recovered in Area 2. Consequently, the Working Group decided to omit the tagging data until a more thorough examination could be conducted, or until more data could be made available.

Examination of the geographical layout of CPUE by fleet, quarter and area, along with the mean size of the fish captured can provide some insights into how bigeye tuna move within a typical year. Consider young of the year recruits spawned in the first quarter of the year in the Gulf of Guinea. The CPUE for the purse seine is at its highest at that time, likely due to high catches of age_1 fish that were spawned the previous year (**Figure 15, top, PS-FAD**). The CPUE declines from quarter one to quarter three, presumably as the previous year's cohort progress through natural mortality, fishing mortality, and migration. The CPUE then increases in quarter four as the current year's cohort recruits into the fishery. This scenario is also supported by the mean length information. The mean length of both the free school (**Figure 15, bottom, PS-FREE**) and FAD purse seine fisheries increases across quarters one, two, and three as the previous year's cohort grow in weight. Then, in the fourth quarter the mean decreases as the smaller current year's cohort (age_0) recruits into the fishery.

As the CPUE in the Gulf of Guinea drops from quarter 1, to 2, and to 3, the CPUE for the baitboat fishery in the Azores (Area 1) increases (**Figure 15, BB-AZ**), indicating that bigeye tuna are moving into that areas. According to the mean quarterly CPUE there are perhaps some resident there year around fish, but new fish arrive abruptly in the second quarter. The decrease in mean size suggests that the newly arriving fish are smaller than the year around residents. The fish then migrate out of that area in quarter three and area almost entirely out by quarter 4. Also in quarter 4 the mean size increases again to the level consistent with the mean size of the resident fish. During this same period, the CPUE from the longline fisheries is increasing steadily as the year progress. Indices for the longline fleets operating in Area 1 peak in the fourth quarter while those operating in Area 3 peak in the third quarter. Longline quarterly CPUEs in the core fishing area (Area 2) are relatively consistent across all quarters, suggesting that not all fish migrate every year. These migration patterns are very consistent with those described in Lam et al. 2014.

3. Assessment Model Configuration

A complete matrix of the observational data used in the stock assessment is shown in **Figure 16**. The SS model structure was based loosely on the MFCL configuration presented by Miyabe (2005) and used in the ICCAT 2010 stock assessment meeting. The time frame for the model was 1950-2014, with the assumption that measurable fishing on the stock began in 1950. With a mind towards consistency and time constraints, the fleet structure was maintained (**Table 1**). The configuration included four, three month seasons, to accommodate year around spawning, and three areas. Information regarding sex composition of the catch was very sparse; consequently only one sex was modeled. A total of 11 ages (including age 0) were modeled.

3.1 Biological Parameters

Morphometric and Reproduction. Weight of bigeye tuna in kilograms was estimated from total length in centimeters as:

$$Wt = (2.396\text{E-}05) * TL^{2.9774}$$

Fecundity was modeled as a direct function of female body weight. The maturity schedule used was adopted from previous assessments: 0% for ages 0-2, 50% for age 3, and 100% for ages 4-10 (**Figure 17**).

Natural Mortality. The data preparatory Working Group reevaluated natural mortality assumptions used in the VPA and SS. The working group no longer prefers the former natural mortality vector (Age 0-1 = 0.8, Ages 2+ 0.4) and recommended the use of a Lorenzen (2005) natural mortality function developed by the group in 2009, and confirmed in 2015 (**Figure 18**). Age-specific M was derived using a Lorenzen (2005) function with the reference M = 0.2794 over the "fully selected" age classes (1-15). The reference M was approximated using a maximum age of 15. The M vector was developed using the Hallier *et al*. (2005) growth curve. Vectors that examine sensitivities to higher or lower M were obtained by increasing or decreasing the target M by 25% (discussed below).

3.2 Stock Recruitment

A Beverton-Holt stock recruitment relation was used to model the number of recruits as a function of spawning stock biomass. Virgin recruitment (*R0*) was freely estimated and steepness (*h*) was either fixed at a value 0.70 or freely estimated. Annual variation in recruitment (*sigma-r*) was fixed at 0.60, a value borrowed from standard convention. The estimated total annual recruitment was distributed equally between the four seasons (i.e. 25% each). Recruitment by each of the three areas was estimated such that Area 1 and Area 3 received equal amounts of recruits and the percentage going to Area 2 was estimated within the model, informed by the landings, CPUE, and length information. Recruit distribute by season and area remained constant each year. Deviations in annual recruitment were estimated from 1974 to 2013.

3.3 Selectivity

Length-based selectivity was estimated for each of the fifteen fleets. Fleets 1-5 (purse seine and bait boat), fleet 9 (northern bait boat), and fleets 10-15 (longlines) were modelled with a five-knot spline function, which allowed for dome-shaped selectivity. Fleets 6-8 (bait boat) were modelled with a double normal function, which also allowed dome-shaped selectivity. The cubic spline function was chosen to capture the bimodal shape of the length composition data (i.e. a mixer of very small and very large fish).

Age-based selectivity was also incorporated. For the purse seine fleets (fleets 1-4) a single, age_0 selectivity was estimated with all other ages being fixed at full selectivity. In this way, the assumed natural mortality of age_0 fish becomes quite important. The assumed natural mortality of age_0 fish will be a direct determinant on the selectivity (and thus fishing mortality) on these fish, which is fully accounted for by the purse seine fleets. For all other fleets (fleets 5-15) age_0 were assumed to have zero selectivity with all other ages being fully selected.

3.4 Data Weighting

The standard deviations of each of the CPUE time series were standardized but with the year-to-year variations maintained. This was accomplished by set setting the year with the minimum standard deviation to 0.20 and making all other years relative to the minimum year. All CPUE time series lambdas were set to 1.0 for all runs. No variance reweighting was attempted with the CPUE.

The model configuration consisted of a total of 111 length bins over approximately 40 years. This makes for a configuration in which a great deal of the negative log-likelihood is made up from the fit to the length information. Indeed, in trial runs, nearly 90% of the total likelihood was attributable to the length information. This makes the selection of the effective sample size on the length information quite important. If set too high, the model fit will be out of balance between the length information and other observational data (i.e. CPUE). The effective sample size was chosen post-model fit such that it was balanced with the estimated effective sample size. The effective sample size of the length compositions for each fleet was adjusted so that the effective sample size working values were equal to their estimated values with a maximum allowed of 100 samples. Two iterations were conducted, which was enough to stabilize the values for all but one fleet. Year-to-year variation in the effective sample sizes were not possible due to an unknown number of samples being taken each year.

3.5 Candidate Models

Three candidate model configurations and associated assumptions were considered for the base model:

> **Model_10**: This model configuration assumed asymptotic selectivity for all of the six longline fleets.
> **Model_11**: This model configuration assumed asymptotic selectivity for the longline fleets in Areas 1 and 2 (fleets 10, 12, 13, and 15) and allowed the longline fleets in Area 2 (fleets 11 and 14) to be dome-shaped.

Model_11h: The same as Model_11 but with steepness estimated.
Model_12: This model configuration allowed all six longline fleets to have dome-shaped selectivity.
Model_12h: Same as Model_12 but with steepness estimated.

3.6 Selection of a Base Model

Over the last five years, the European purse seine FAD fishery (fleets 4) and the non-Japanese longline fishery (fleet14) made up 25% and 30% of the total bigeye landings, respectively, for a total of 55 percent. Based on the majority of the landings coming from these two fleets, it seemed prudent to favour capturing the characteristics of these two fleets, perhaps over the remaining 13 fleets.

Despite the apparent visual similarity between the length compositional data of all six longline fleets (fleets 10-15), the model was able to adequately fit the lengths of fleets 10 and 12, and fleets 13 and 15 with a simple logistic function, however, a five knotted spline function was necessary to effectively fit fleets 11 and 14, the core fishing area (Area 2) fleets (**Figure 19**). By definition the logistic function fits an asymptotic selectivity function which is very often assumed by ICCAT Working Groups for longline fleets. However, the spline function fit resulted in a dome-shaped selectivity function.

Model 10 resulted in the highest likelihood values (i.e. worst fit to the observational data) (**Figure 20**). Even though this model has the least number of parameters, the likelihood was improved by over 10,000 units by adding only 20 parameters, all of which were selectivity parameters. Model 12 had a lower total likelihood than Model 11, but not low enough to justify the additional 16 parameters (**Table 2**).

There is a direct relation between the estimate of L-infinity and the dome-ness of fleets 11 and 14 selectivity. The L-infinity suggests that the mean maximum size of at least 200 cm, but the longline fleet does not see fish this large. Either one believes the large L-infinity or asymptotic selectivity, but the data suggests that both cannot be true. Given the migratory pattern of the species, and the improved fit to the length information, the base model uses the dome-shaped selectivity option.

The movement parameters were not well estimated (see appendix). Also, the movement parameters wanted to keep moving more and more fish into Area 1(?). The recruit distribution was allowed to be estimated and while the estimated values were very close to those previously fixed values, it did not help estimate the movement parameters. While adding the tagging data may have made these parameters more estimable, given the nature of the tagging data they likely would not have been accurate estimates.

Six parameters were correlated above the selected 70 percent threshold (**Table 4**). The two most highly correlated parameter pairs were the R0 and the steepness parameters (-0.91) and the growth function k value and L infinity (-0.90).

The model chosen as the base model was Model_11 with steepness being estimated. The reasons this model configuration was chosen as the base were: (1) on first principals, based on the migratory patterns of the fish, it made sense that the largest fish might not be fully available all year in Area 2; (2) This configuration fit the length composition of the fleets in the core area the best, perhaps due to the migratory patterns; (3) unlike Model_12, it was able to fit the entire range of steepness for the profile analysis.

From this point forward, or unless otherwise mentioned, this document will refer to the base model, Model_11h (with steepness being estimated).

3.7 Base Model Fits

Selectivity. First attempts to fit selectivity functions used the double-normal function. However, due to the extremely peaked nature of the length compositions the spline function, with five joints, was found to be far superior for the purse seine fleets **(Figure 21)**. The spline function was also the only function able to capture the bimodal shape of the purse seine length compositions. The baitboat fleets required a mix of double-normal and spline functions (**Figure 22**). The longline fleets from Area 1 and Area 3 were assumed asymptotic by using the logistic function, as it was thought that these fisheries should be catching the largest fish available in the population, but this assumption is open to debate. The longline fleets in the core area (Area 2) used a spline fit (**Figure 23**) because of the improved fit and for the notion to allow larger fish not to present at all times due to annual migration.

Stock recruitment. The estimated annual recruitment deviations were "well behaved" **(Figure 24)**. The largest negative deviation came in the final year of the estimates (2013). Usually, the last year of recruitment (and/or deviations) is not thought to be very reliable as that year class has not been observed for very long. However, in the case of bigeye, since the purse seine fishery catches age_0 and age_1 the 2013 may be relatively reliable. In an effort to get the movement parameters off their bound the distribution of recruits between areas was allowed to be estimated. The initial distribution assumed from the previous assessment work was 75% in Area 2 and 12.5% in both Areas 1 and 2. When allowed to be estimated the result was 60% in Area 2 and 20% in both Areas 1 and 2. Note that even though the distribution of recruits was estimated, Areas 1 and 3 were fixed to be equal. It should further be noted that no time varying parameters were used for this. Although the biology would suggest year-to-year variation, there was no data to support any type of hypothesis testing.

The estimate the steepness parameter of the Beaverton-Holt stock-recruitment curve (0.711, SD = 0.019) was within the range of the Working Group had asked to see (0.60 – 0.80). This value of steepness was later profiled on and the results indicated a reasonable fit to the parameter (but not necessarily an accurate one, see below).

Fit to Indices of Abundance. The fit to the overall, long term, trend in the indices was reasonable fit. However, where the fit may be lacking could easily be due to year-to-year variation in migratory patterns. As noted above, it has long been recognized that annual variation in oceanographic features can modify the timing and patterns of bigeye tuna movements. But without high quality tagging data or known mechanisms of movement it is difficult to attempt to incorporate variations in migration into the assessment model. However, while capturing these variations may improve the fit to observational data, it may or may not improve the models estimate of overall stock status.

The purse seine index was provided late in this assessment process and did not have the advantage of Working Group review during the Data Preparatory meeting. Thus, its inclusion is likely best viewed as provisional. The general trend of fit to the purse seine and baitboat CPUE was fit, but year-to-year variation was not captured as well (**Figure 25**). As discussed above, the large drop in the Azores baitboat CPUE coincides with a switch in sign of the AMO. It has been noted in previous years that this could be caused by changing oceanographic conditions and thus may not be indicative of true stock abundance.

The most recent trends in the Japanese longline CPUE were a bit contradictory. While the CPUE in Area 1 showed a large drop in the most recent years, the CPUE in Area 2 actually showed an increase (**Figures 26)**. One explanation for this contradiction is fish not migrating out of Area 2 and into Area 1 at an average rate. The fit to the Area 3 CPUE is better, but likely because of its relatively consistent trend.

The fits to the "other" longline fleets all showed similar trends in fits: and under estimate at higher levels of biomass. This can be seen in the residual patterns deviating from the straight line at high "observed index" values **(Figure 27)**. Some of this pattern may be due to a potential "learning curve" during the first part of the fishery.

Fit to Lengths. Overall, when examined as an aggregate across all time, the fit to the length compositions was quite good. When the fits are examined for lengths aggregated by quarter, trends in lack-of-fit can be seen. For example, the peak of the lengths for fleet 4 is under estimated in the first two quarters and then over estimated in the last two quarters (**Figure 28**). Very likely this is due to a combination of two factors. One, the selectivity is length-based, which does not change as the fish grow. Second, bigeye tuna growth very rapidly during the early part of their lives. Consequently, fish grow "through" the length-based selectivity curve as the year progresses. One solution to this would be to use quarters as years in the model. That is, to configure the model so that every 4 months is seen as a year rather than a quarter.

***Fit to mean size at age*.** The fit to the mean size-at-age information was fairly good with no obvious biases **(Figure 30)**. As mentioned earlier, fitting to the estimated mean size-at-age is not the ideal method, but given the lack of direct observations, this seemed like a viable way to attempt to capture the variation between all recent age and growth studies done in the Atlantic.

In an effort to better match the estimated size-at-age at age_0 with the observations of daily ring counts (data was not able to be fit within the model), the observations of daily age from Hillier et al. (2005) for fish between the ages of 0.0 and 1.0 years were overlaid on to the estimated selectivity curve from the purse seine fishery (fleet 4) from which the samples came (**Figure 31, top**). This plot shows very clearly that the vast majority of fish under the major portion of the selectivity curve are age_0 fish (blue dots) and are centred at around 48 cm. However, the length frequency of age_0 fish from the model estimate of age_0 (born in quarter 1 and captured in quarter 4) is only approximately 34 cm. Knowing that the size of fish less than age_1 is not always well estimated in the SS

model, I attempted to "calibrate" the size-at-age within the model by fixing the size at age 0.5 years such that it matched the observed size at age_0.5 from the Hillier *et al.* (2005) data. With the adjusted growth function, the purse seine fishery selectivity, the observed size of age_0.5, and model estimated size at age_0.5 are now all centred on 48 cm (**Figure 31, bottom**). This is a critical adjustment as it makes much of age_0.5 now fully vulnerable to the purse seine fleet as it seen at the bottom of Figure 31. This growth adjustment (and only this adjustment) is made in Model_20h, which will be presented at the assessment meeting, but not discussed any further in this document.

3.8 Base Model Diagnostics

Residual Mean Square Error. The CPUE time series that was most consistent with the rest of the observation data (i.e. had the lowest residual mean square error) was the Japanese longline fleet in Area 2 (r.m.s.e = 0.35). Very close in consistency was the Japanese longline fleet CLUE from Area 1 (r.m.s.e = 0.36) (**Table 3**). The CPUE time series least consistent with the remaining observational data was the Uruguayan longline CPUE (r.m.s.e = 1.12).

Profile Analysis. A profile analysis was performed on the steepness parameter of the stock-recruitment function. Overall, the fit to the parameter showed a minimum likelihood at 0.70, which was in line with the estimated value of 0.71 (**Figure 32).** The information contained in the CPUEs tended to draw the estimate to low values, while the information in the length compositions and the size-at-age tended to draw the estimate to high values. The similarity in the shape and magnitude of the "Total" curve and the "Lengths" curve suggests that the overall estimate of steepness may be being driven a great deal by the length information.

When the profiling is broken down by individual component it can be seen that not all of the CPUEs tended toward low steepness. Some tended to lead towards a common minimum of approximately 0.6 (**Figure 33**). The odd shape of fleet 11 has no obvious explanation. Nearly all the length compositions tended towards higher values of steepness (**Figure 33**). Fleet 7 was the exception with no obvious explanation for the odd shape. The size-at-age information was either non-informative or tended towards higher values (**Figure 33**).

Jitter. An exercise was performed were the starting values of each estimated parameter were randomly "jittered" by a fraction of 0.01 and the entire model refit. This was repeated 75 times. The jitter exercise resulted in several minimum –logLikelihood values with a range of approximately 50 likelihood units (**Figure 33**). This is neither an ideal outcome nor a reason to abandon the model. Fixing some of the parameters that are not well estimated may help resolve this issue.

3.9 Trends in Stock Abundance

Spawning biomass and recruitment. The trends in spawning stock biomass and recruitment from the base model were generally steadily declining (**Figure 34**). The final few years did show this decline beginning to taper off, but no increases were apparent. It needs to be noted that the last year of recruitment (2014) was not estimated, but rather came directly from the stock-recruitment curve because a deviation was not estimated for that year. This should be kept in mind should any forecasts be done with this model. That is, it may make the forecasts overly optimistic if future recruitments are expected to jump from all-time lows immediately to those estimated from the stock-recruitment function.

Catch at Age and Yield-per-Recruit. The overall catch at age has, and continues to, move from mainly older fish to younger fish. A jump in proportion of the catch being made up of age_0 and age_1 fish is apparent in the early 1990's when the purse seine fishery on FADs became a major fishery **(Figure 35).** The mean age of catch has also dropped from approximately 3.5 years in the 1960 to approximately 2 years in recent times. This has led to decrease in the yield-per-recruit as the curve has begun to bend over the peak.

As far back as 1994 it was noted that the manner in which the fishery was being prosecuted was not allowing for the maximum yield-per-recruit (YPR):

From SCRS_ 94-95**:** *"The analysis of yield per recruit for bigeye tuna suggests that reducing fishing mortality of juvenile fish up to age 2, and simultaneously increasing the rate of fishing mortality on adult fish, could increase the yield per recruit."*

Now, twenty years later, the gradual and steady shift in the catch coming less from the longline fishery and more from the purse seine fishery has continued, exacerbating the decline in efficiency of the fishery.[2]

References

Brown, C. 2005. An overview of Atlantic bigeye tuna (*Thunnus obesus*) growth studies and implications for age-structured stock assessment. Collect Vol. Sci. Pap ICCAT. 57, 94-114.

Eveson, J. P., Million, J., Sardenne, F., & Le Croizier, G. (2015). Estimating growth of tropical tunas in the Indian Ocean using tag-recapture data and otolith-based age estimates. Fisheries research, 163, 58-68.

Hallier, J-P, B. Stequert, O. Maury, F-X. Bard. 2005. Growth of bigeye tuna (*Thunnus obesus*) in the eastern Atlantic Ocean from tagging-recapture data and otolith readings. ICCAT Col. Vol. Sci. Pap. 57(1):181-194.

Lam, C. H., Galuardi, B., & Lutcavage, M. E. (2014). Movements and oceanographic associations of bigeye tuna (*Thunnus obesus*) in the Northwest Atlantic. *Canadian Journal of Fisheries and Aquatic Sciences*, 71(10), 1529-1543.

Minte-Vera, Carolina V., Mark N. Maunder, Alexandre M. Aires-da-Silva, Kurt M. Schaefer, and Daniel W. Fuller. 2015. Evaluation of including the cost of reproduction in a growth model for bigeye tuna in the eastern Pacific Ocean, and the effect on stock assessment results and management advice. Scientific Advisory Committee Sixth Meeting. (2015).

[2] Appendices 1 and 2 can be consulted in soft copy only and are not attached to this publication. These are available for consultation under Coll. Vol. Sci. Papers. #72 in the ICCAT webpage publication menu.

Table 1. Fleet definitions used in the SS assessment model.

Fishery	*Gear*	*Nation*	*Area*	*Years covered*
1	PS	France, Spain and others (early)	2	1965 - 1985
2	PS	France, Spain and others (transition)	2	1986 - 1990
3	PS	France, Spain - Free School	2	1991 - 2014
4	PS	France, Spain - FAD	2	1991 - 2014
5	BB	Ghana BB+PS	2	1973 - 2014
6	BB	Other tropical nations (south)	2	1962 - 2000
7	BB	Other tropical nations (north, early)	2	1965 - 1979
8	BB	Other tropical nations (north, late)	2	1980 - 2014
9	BB	Potugal, Spain (North Islands)	1	1965 - 2014
10	LL	Japan	1	1961 - 2014
11	LL	Japan	2	1961 - 2014
12	LL	Japan	3	1961 - 2014
13	LL+Uncl	Others (US. Chinese Taipei, etc.)	1	1968 - 2014
14	LL+Uncl	Others (US. Chinese Taipei, etc.)	2	1966 - 2014
15	LL+Uncl	Others (US. Chinese Taipei, etc.)	3	1966 - 2014

Table 2. Likelihood for each of the candidate models, with and without steepness estimated, by each data component in the model.

	Model_10	Model_10h	Model_11	Model_11h	Model_12	Model_12h
NPARMS	128	129	148	149	164	165
TOTAL LIKELIHOOD	46,969	45,823	37,393	37,393	36,994	36,983
Catch	16.4094	17.012	3.90E-12	3.94E-12	3.86E-12	3.56E-12
Equil_catch	0	0	0	0	0	0
Survey	1,368	1,471	686	691.19	710	672
Length_comp	39,877	38,885	31,190	31188.3	30,970	30,968
Size_at_age	5,714	5,462	5,536	5532.44	5,330	5,360
Recruitment	-6.79	-10.65	-18.74	-18.7526	-16.76	-16.69
Forecast_Recruitment	0	0	0	0	0	0
Parm_priors	0	0	0.002	0.002	0.010	0.010
Parm_softbounds	0.035	0.039	0.034	0.034	0.037	0.037
Parm_devs	0	0	0	0	0	0
F_Ballpark	0.015	0.003	0.004	0.003	0.009	0.023
Crash_Pen	0	0	0	0	0	0
steepness =	fixed at 0.7	1.00	fixed at 0.7	0.711711	fixed at 0.7	0.608661

Table 3. Residual mean square error for each of the CPUE indices used in the base model.

Index_variance_tuning_check								
Fleet	Q	N	r.m.s.e.	nput+VarAdj+extr	New_VarAdj			
4_ESFR_FADS2_PS_9114	1.69E-05	96	0.5957	0.2854	0.3103			
9_BB_North1_6514	1.49E-02	104	0.8343	0.3225	0.5118			
10_Japan_LL1_6114	1.14E-03	203	0.7583	0.3139	0.4444			
11_Japan_LL2_6114	1.80E-04	216	0.3640	0.2197	0.1443			
12_Japan_LL3_6114	2.11E-03	214	0.6297	0.2797	0.3500			
13_Others1_LL_6514	4.36E-03	114	0.5319	0.2190	0.3129			
14_Others2_LL_6514	1.83E-04	188	0.3479	0.2160	0.1319			
15_Others3_LL_6114	7.29E-03	114	1.1237	0.6432	0.4805			
Length_comp_Eff_N_tuning_check								
FleetName	Fleet	mean_effN	mean(inputN*Adj)	HarMean(effN)	Mean(effN/inputN)	MeaneffN/MeaninputN	Var_Adj	HarEffN/MeanInputN
1_PS_ESFR2_6585	1	77.32	35	34.27	2.21	2.21	1	0.98
2_PS_ESFR2_8690	2	94.53	54	54.42	1.75	1.75	1	1.01
3_PS_ESFR2_9114	3	45.31	29	29.16	1.56	1.56	1	1.01
4_ESFR_FADS2_PS_9114	4	104.48	64	64.42	1.63	1.63	1	1.01
5_BB+PS_Ghana2_6514	5	33.27	20	20.04	1.66	1.66	1	1.00
6_BB_FisTropS2_6214	6	21.59	14	14.43	1.54	1.54	1	1.03
7_BB_FisTropN2_6579	7	131.24	58	56.91	2.26	2.26	1	0.98
8_BB_FisTropN2_8014	8	82.08	36	36.28	2.28	2.28	1	1.01
9_BB_North1_6514	9	72.28	36	35.67	2.01	2.01	1	0.99
10_Japan_LL1_6114	10	98.74	56	56.25	1.76	1.76	1	1.00
11_Japan_LL2_6114	11	205.67	100	132.25	2.06	2.06	1	1.32
12_Japan_LL3_6114	12	86.99	52	52.48	1.67	1.67	1	1.01
13_Others1_LL_6514	13	84.69	49	49.48	1.73	1.73	1	1.01
14_Others2_LL_6514	14	274.67	100	192.62	2.75	2.75	1	1.93
15_Others3_LL_6114	15	81.57	45	44.71	1.81	1.81	1	0.99

Table 4. Correlated parameters above the selected 70% threshold.

	label.i	label.j	corr
1	VonBert_K_Fem_GP_1	L_at_Amax_Fem_GP_1	-0.90107
2	SR_BH_steep	SR_LN(R0)	-0.91957
3	SizeSel_6P_6_6_BB_FisTropS2_6214	SizeSel_6P_4_6_BB_FisTropS2_6214	0.821067
4	SizeSel_7P_3_7_BB_FisTropN2_6579	SizeSel_7P_1_7_BB_FisTropN2_6579	0.848879
5	SizeSel_8P_3_8_BB_FisTropN2_8014	SizeSel_8P_1_8_BB_FisTropN2_8014	0.924213
6	SizeSpline_Val_1_3_PS_ESFR2_9114_3_BLK4repl_1950	SizeSpline_GradLo_3_PS_ESFR2_9114_3_BLK4repl_1950	-0.75787

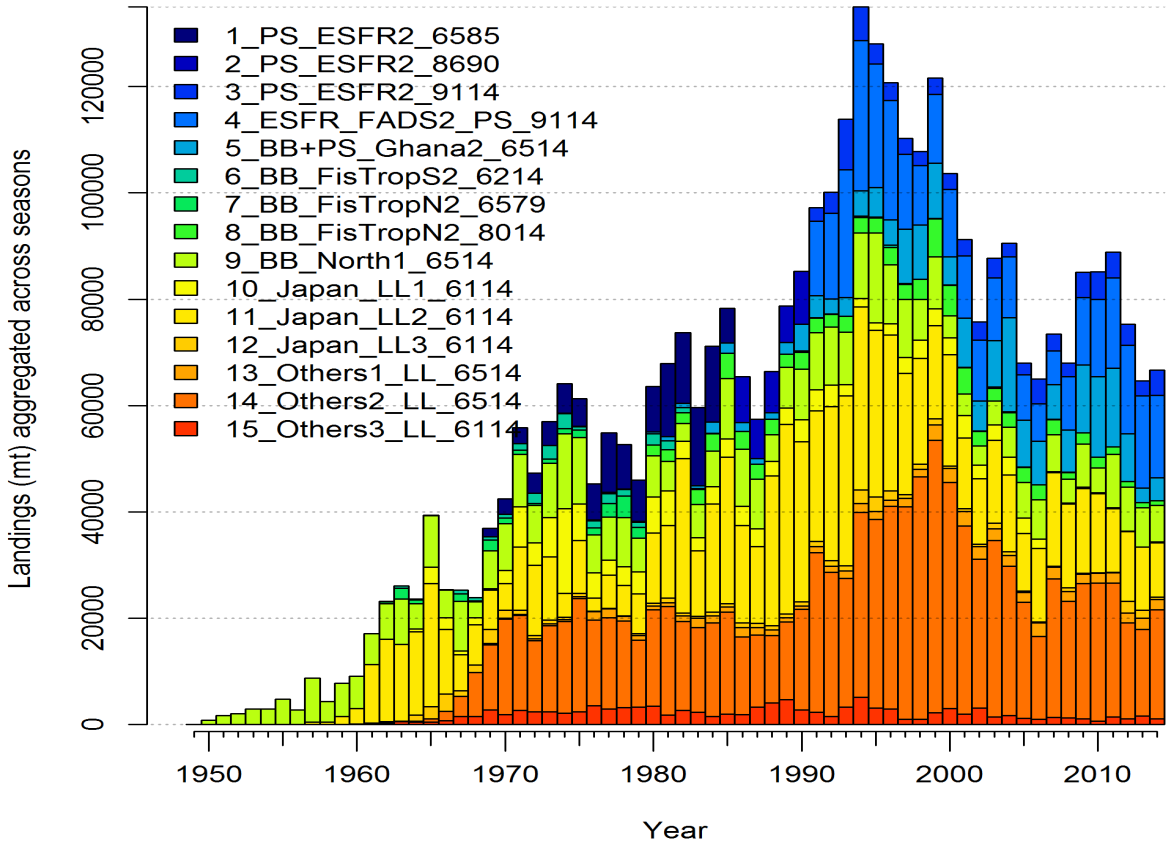

Figure 1. BET landings by major gear group (top) in metric tons and (bottom) as a percentage of the total landings.

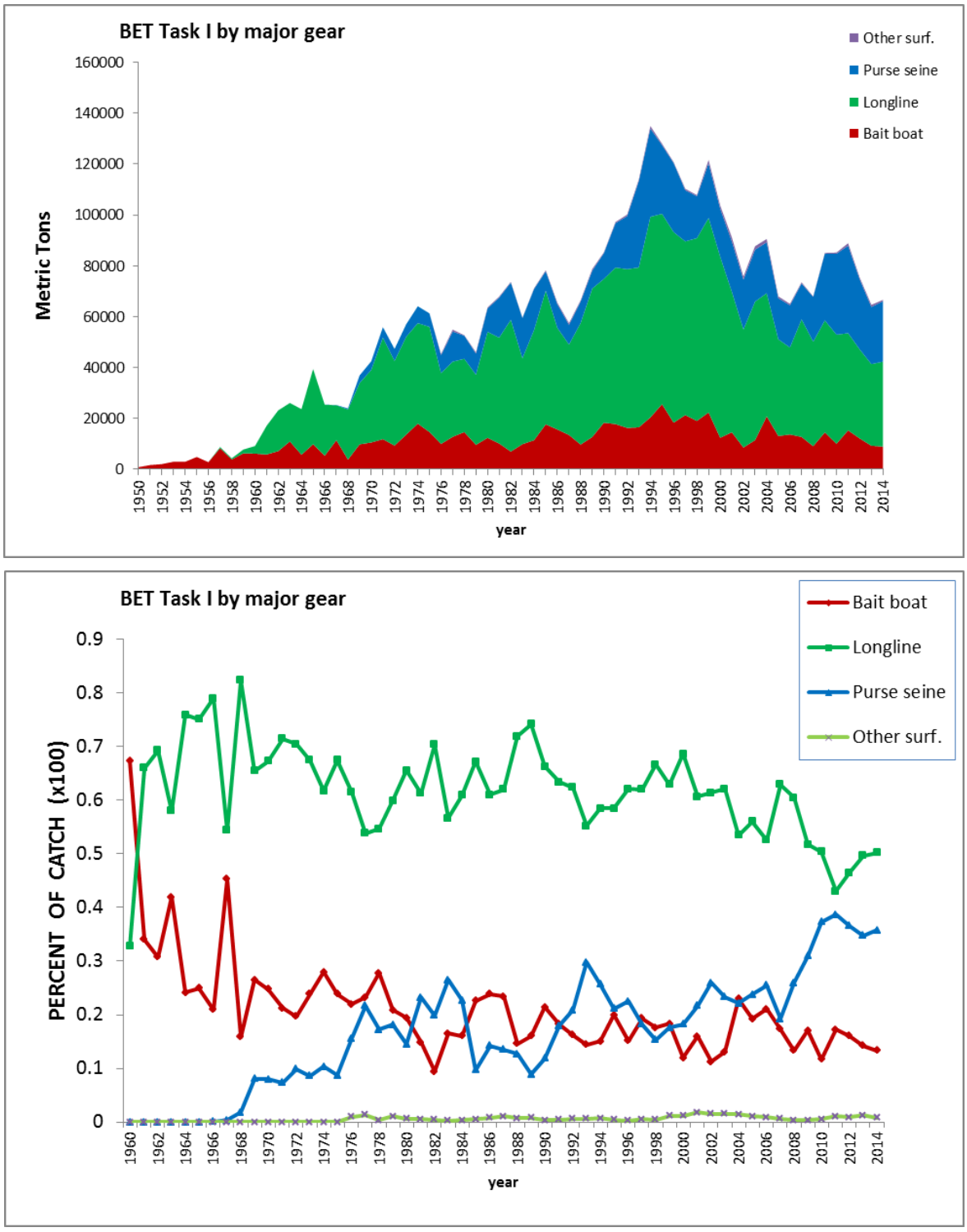

Figure 2. BET landings by major gear group (top) in metric tons and (bottom) as a percentage of the total landings.

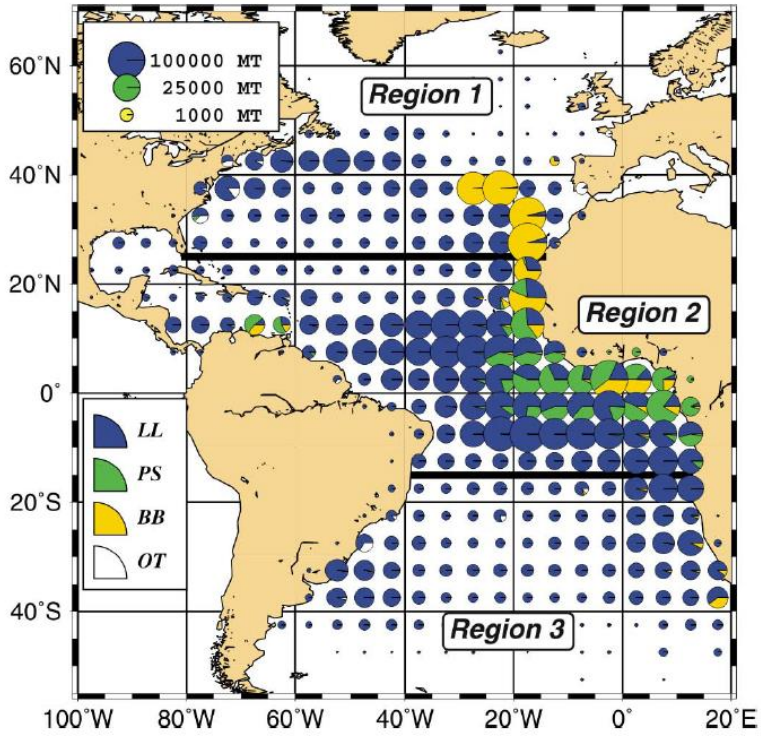

Figure 3. Description of region (delineated by bold horizontal lines) used for SS model, superimposed with catch by fishery accumulated for 1950-2002.

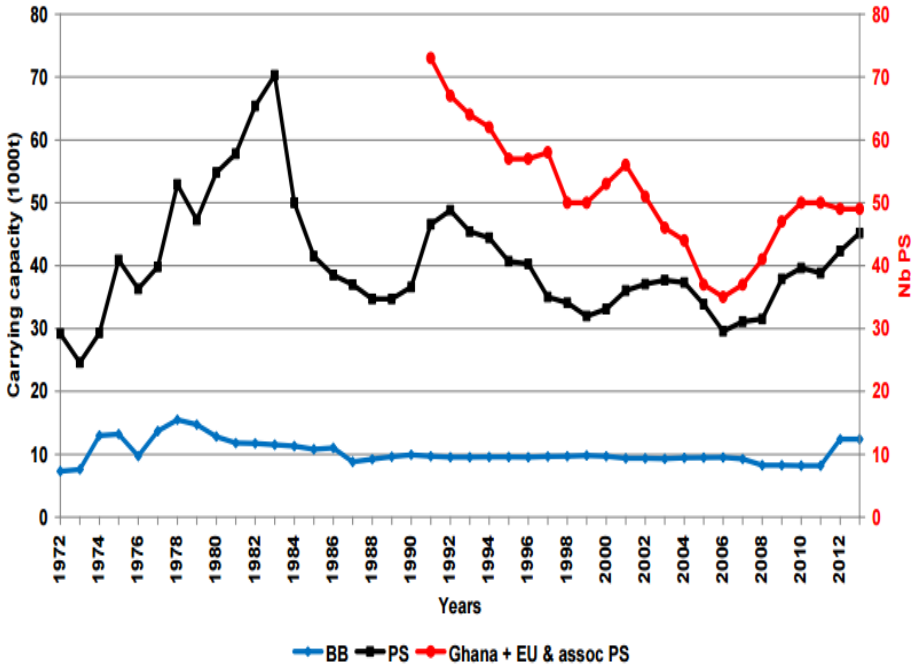

Figure 4. Changes over time in the carrying capacity, corrected by the annual percentage of time at sea, (left axis) for the overall purse seiners and baitboats operating in the eastern Atlantic (1971-2013) and in number of boats for the European purse seiners, associated and Ghanaian fleets (right axis). It is possible that the carrying capacity for some segments of the purse seine fleet was underestimated during recent years (SCRC BienRep/14-15).

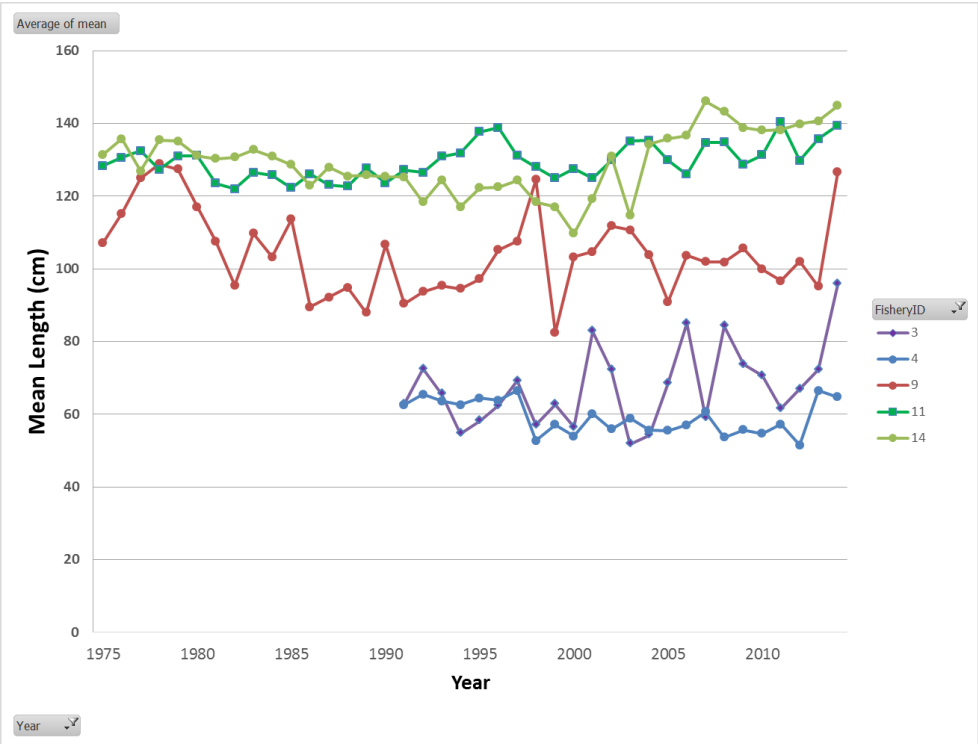

Figure 5. Mean length (cm) of BET landings by major gears and SS fleet: purse seines free schools (fleet 3) FADS (fleet 4); bait boats in north (fleet 9); and Japanese longline in Area 2(fleet 11) and other surface gears Area 2 (fleet 14).

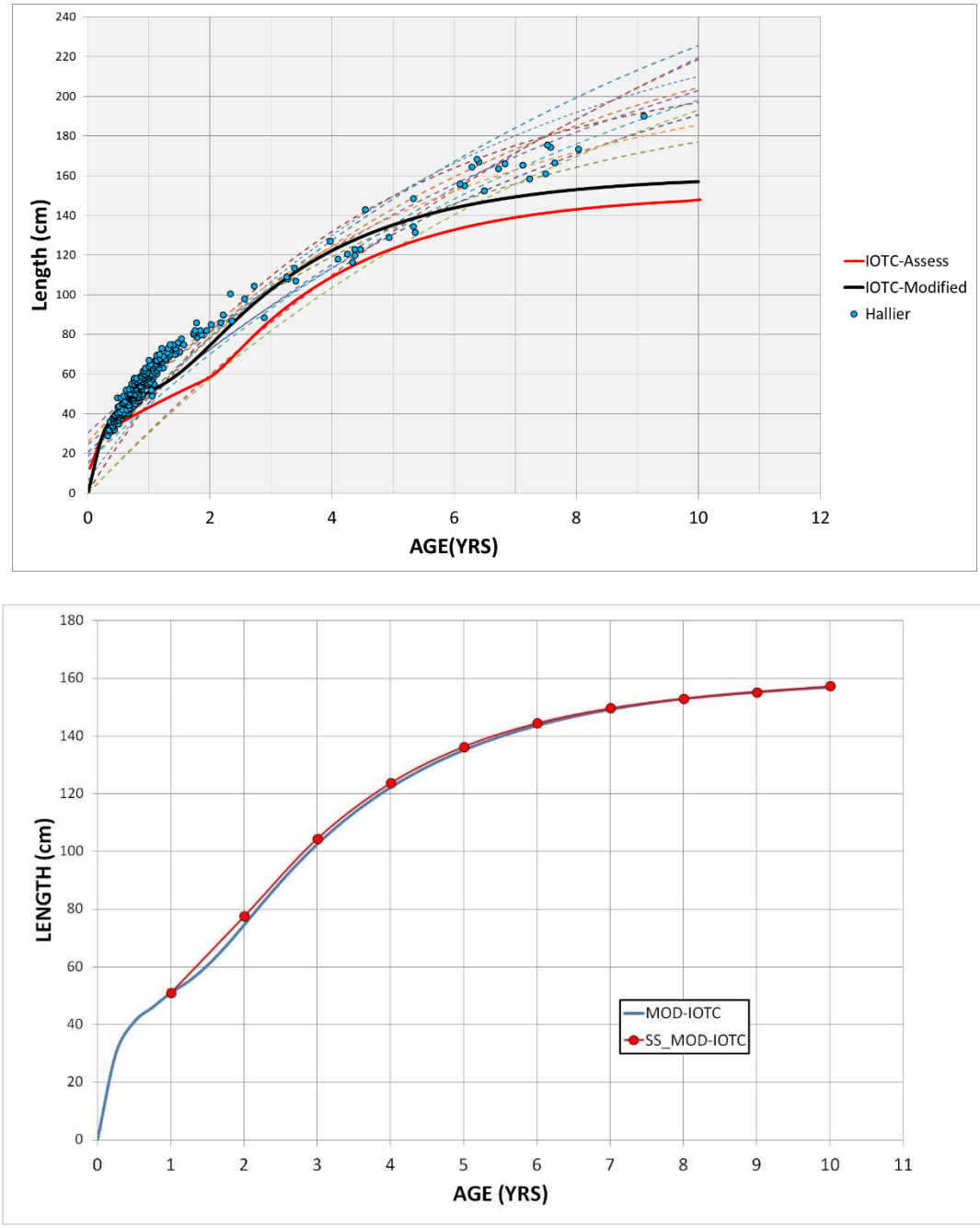

Figure 6. The three growth curves discussed for use in the for bigeye tuna. Top panel, dotted lines are the various curves reported in Brown (2005), the red line the curve used in the IOTC assessment, and the black line the curve suggested by Fonteneau (2015). The bottom panel is the curve suggested by Fonteneau (2015) and the curve designed to approximate it and used in the SS model.

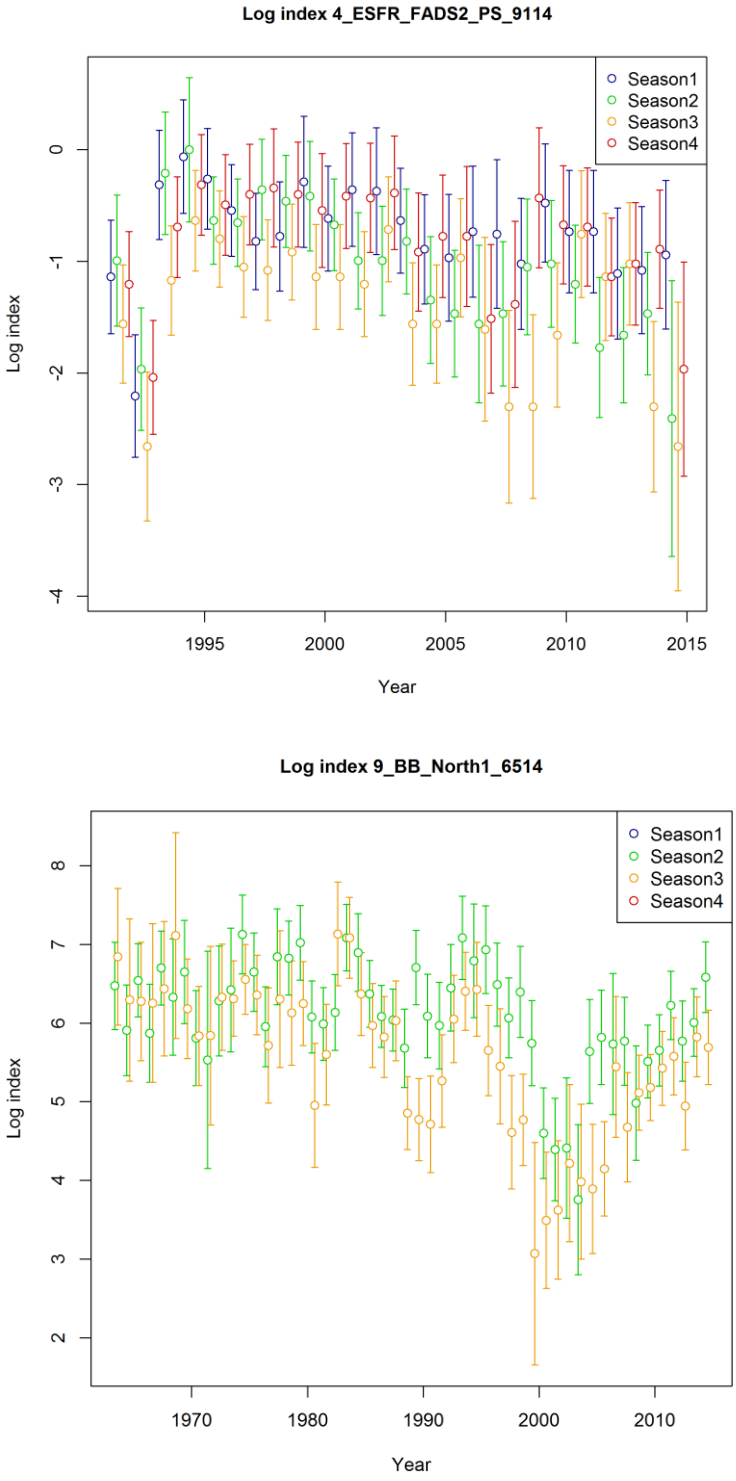

Figure 7. BET landings by major gear group (top) in metric tons and (bottom) as a percentage of the total landings.

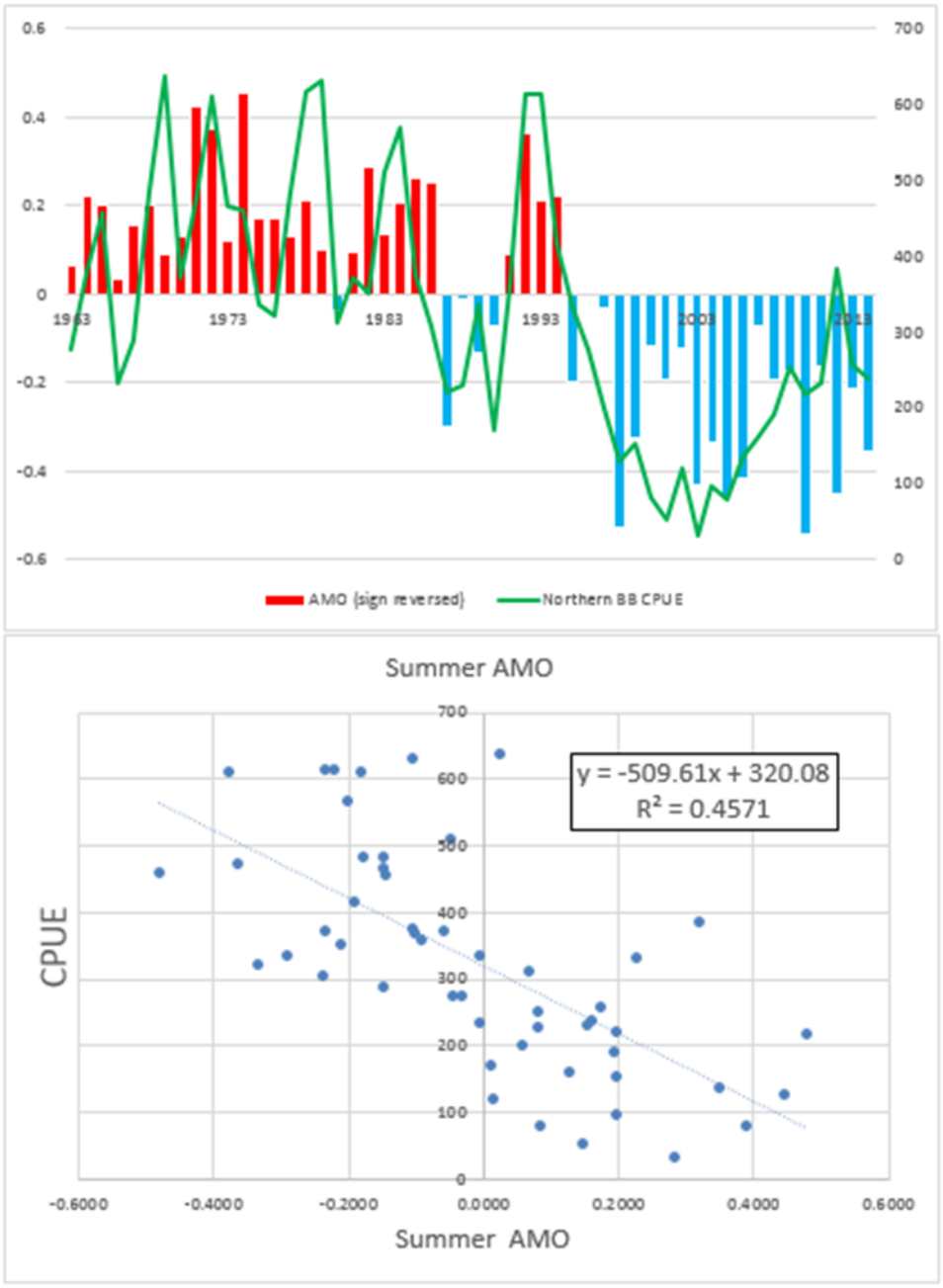

Figure 8. Relation between the Summer AMO (sign reversed for ease of comparison) and the northern bait boat CPUE off the Azores Islands.

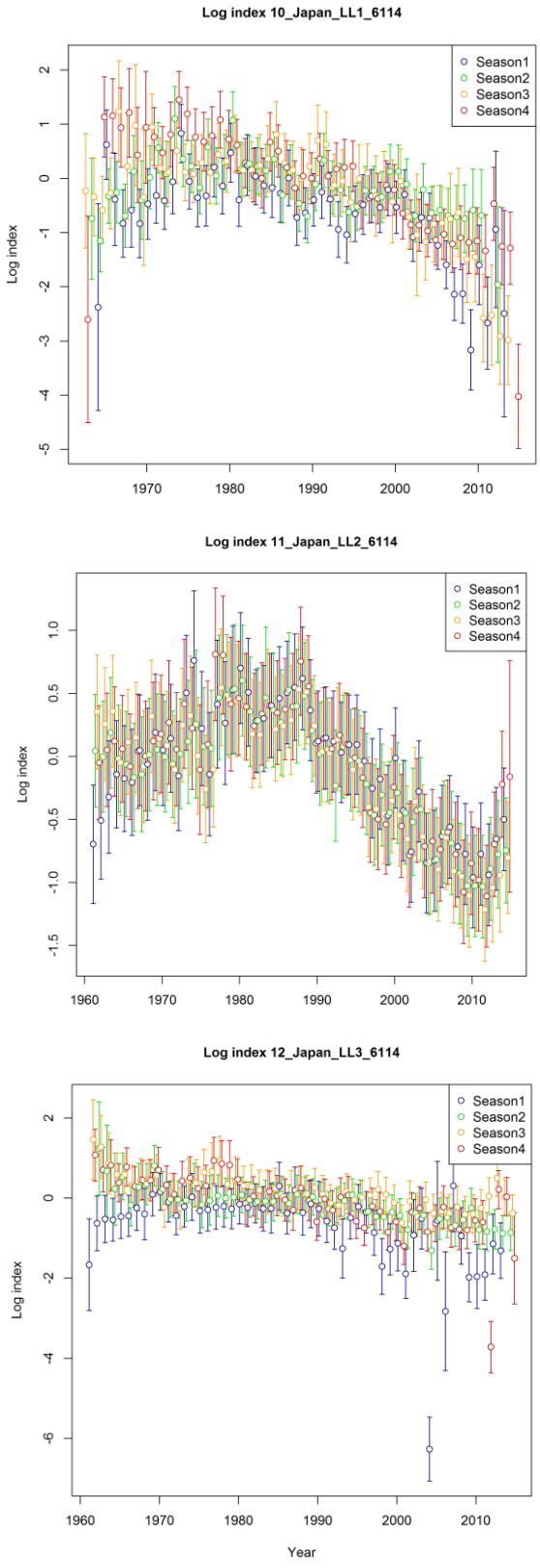

Figure 9. BET landings by major gear group (top) in metric tons and (bottom) as a percentage of the total landings.

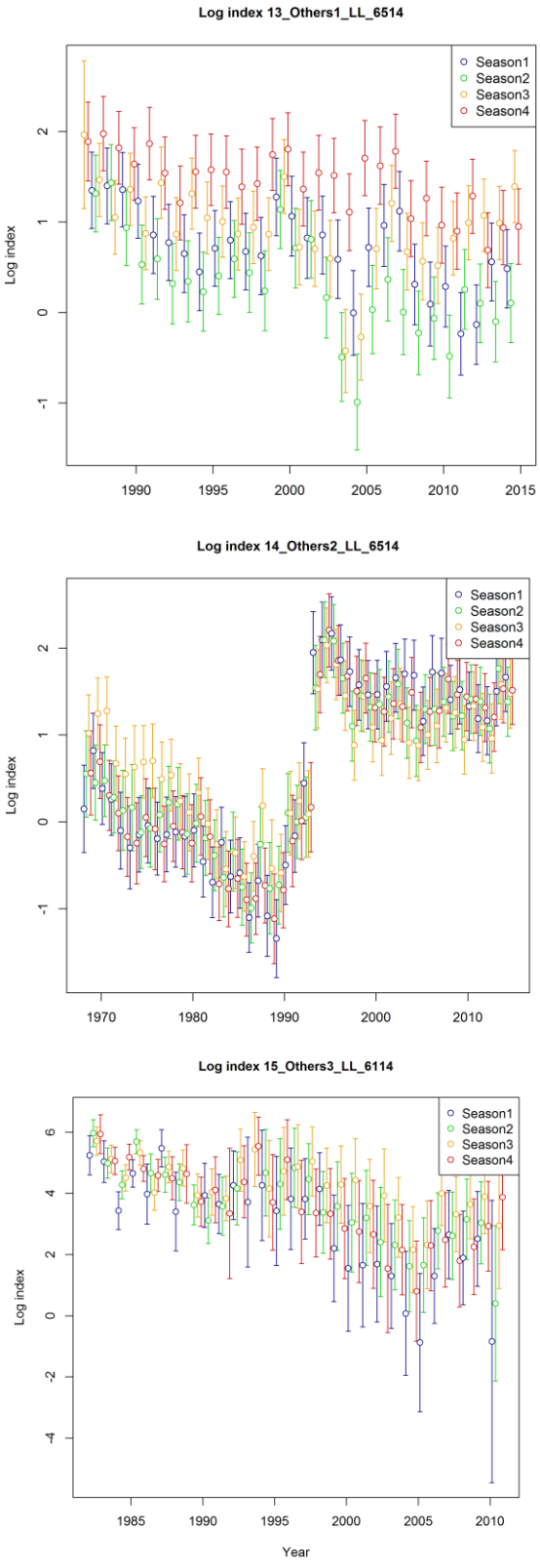

Figure 10. BET landings by major gear group (top) in metric tons and (bottom) as a percentage of the total landings.

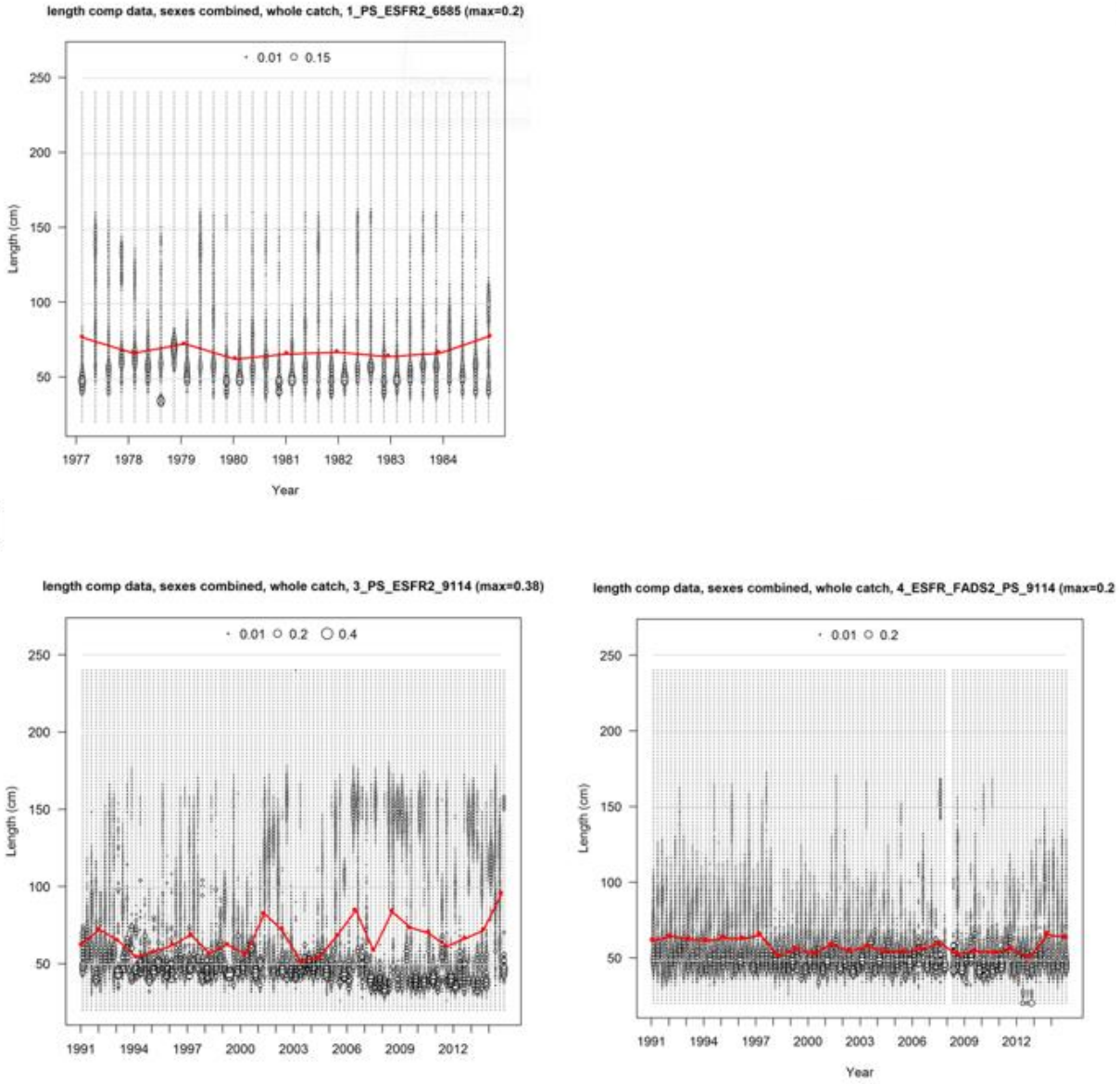

Figure 11. BET length compositions from the four purse sein fleets. Red line indicates the average length by year.

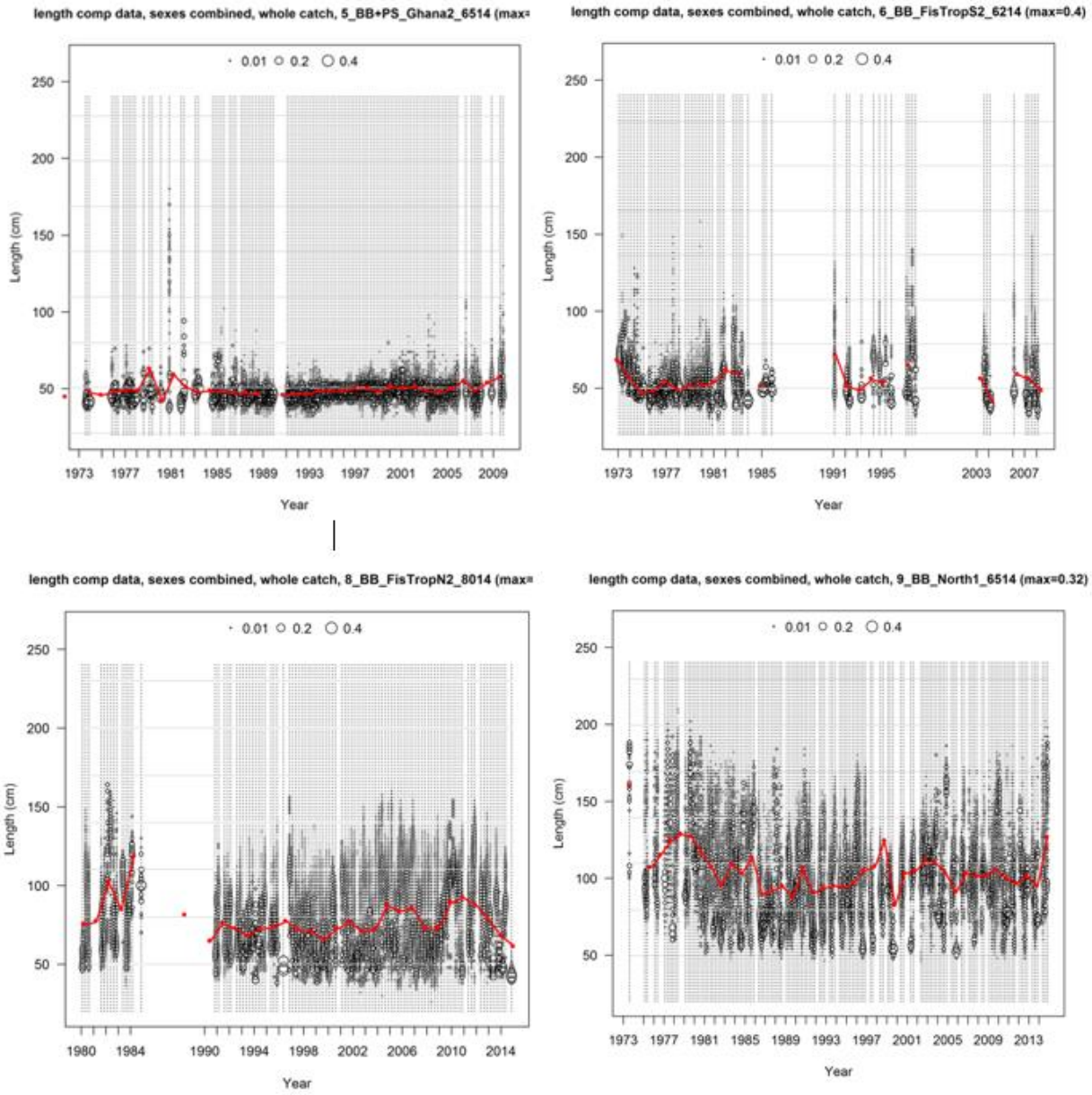

Figure 12. BET length compositions from the four bait boat fleets. Red line indicates the average length by year.

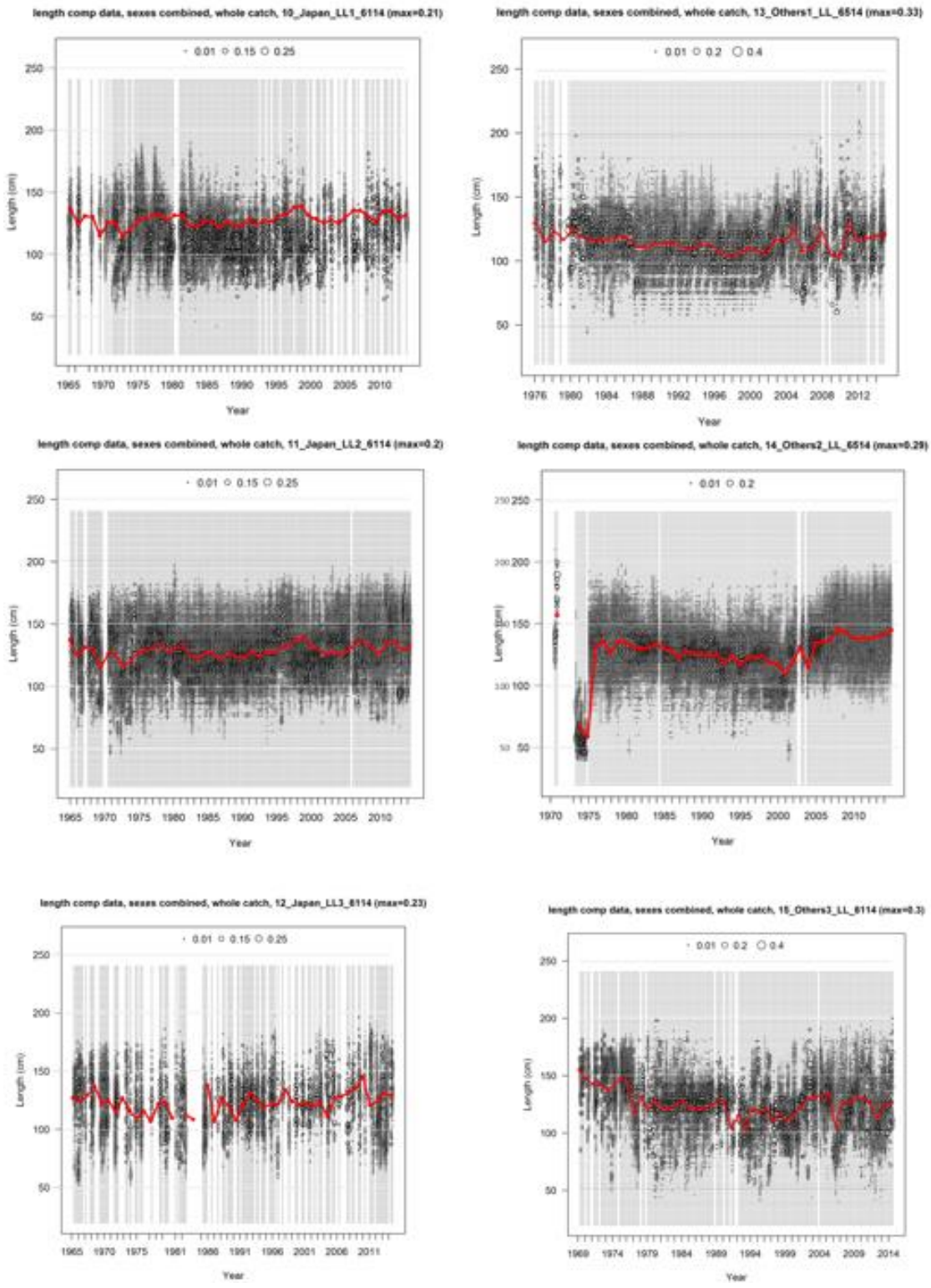

Figure 13. BET length compositions from the six longline fleets. Red line indicates the average length by year.

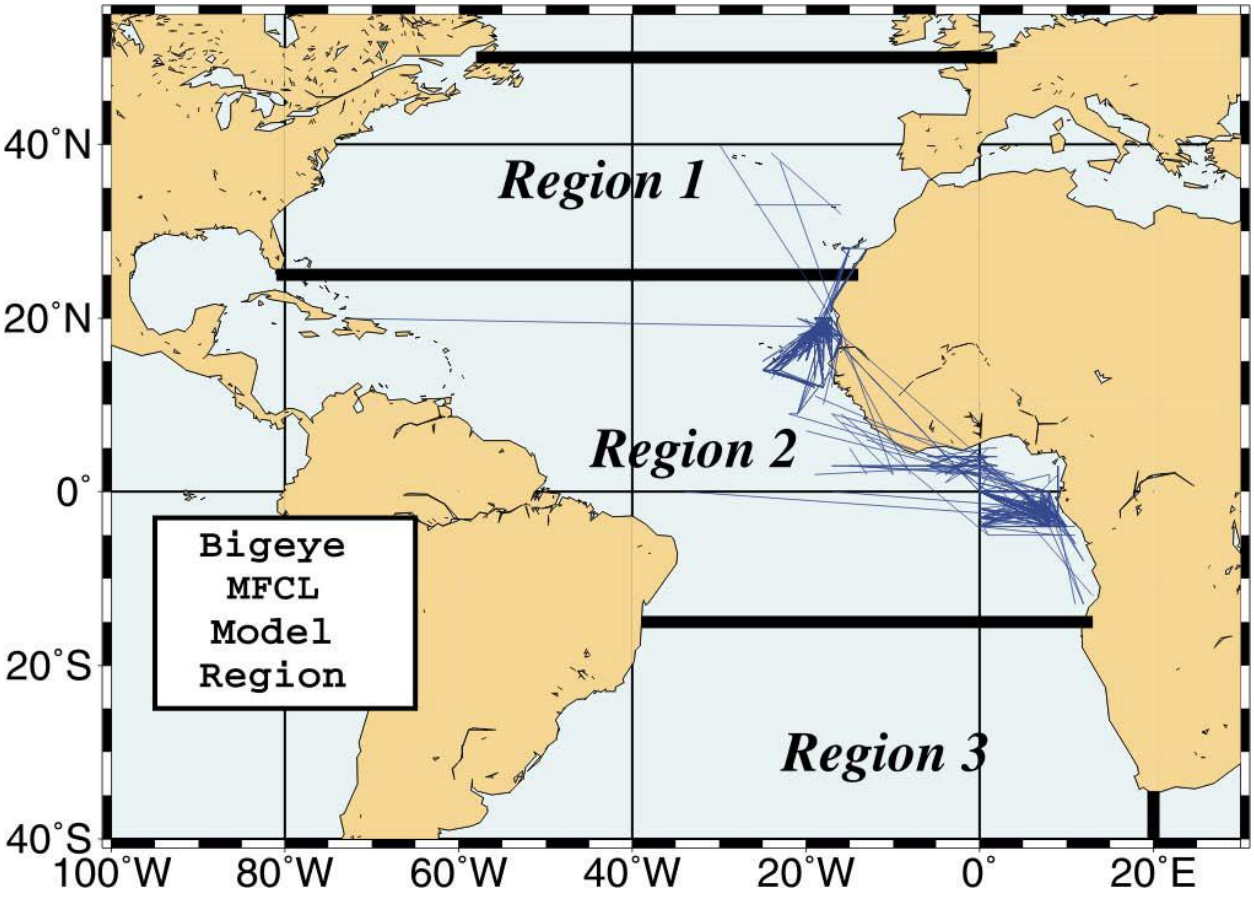

Figure 14. BET tag recovery data available for this assessment. Tagging data was deemed to sparse and not reflective of stock movement to be used as part of the assessment model (from Miyabe 2005).

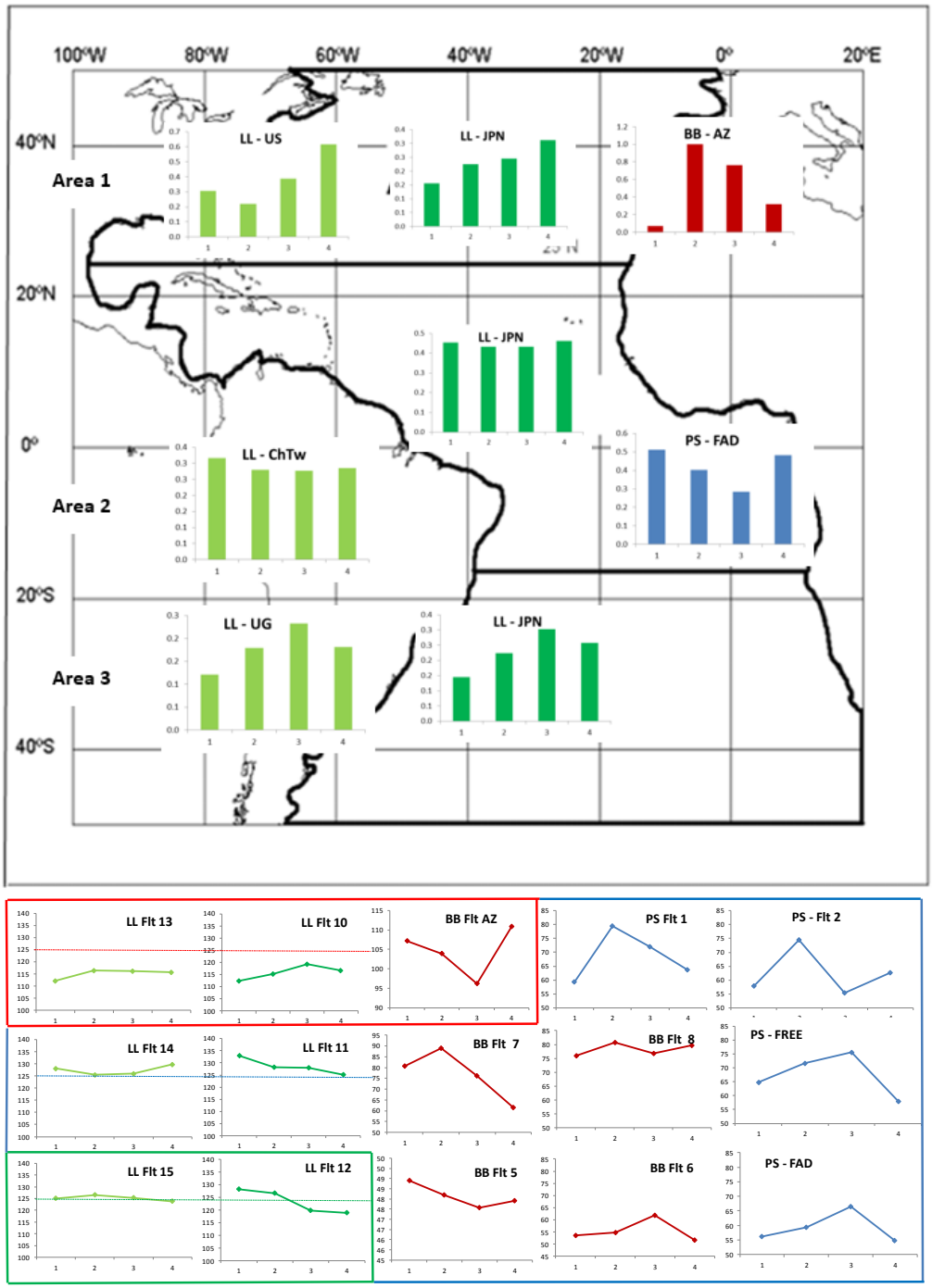

Figure 15. BET (top) CPUE by fleet and quarter averaged over all years (for those fleets with CPUE), and (bottom) mean length by fleet and quarter (for all fifteen fleets) averaged over all years.

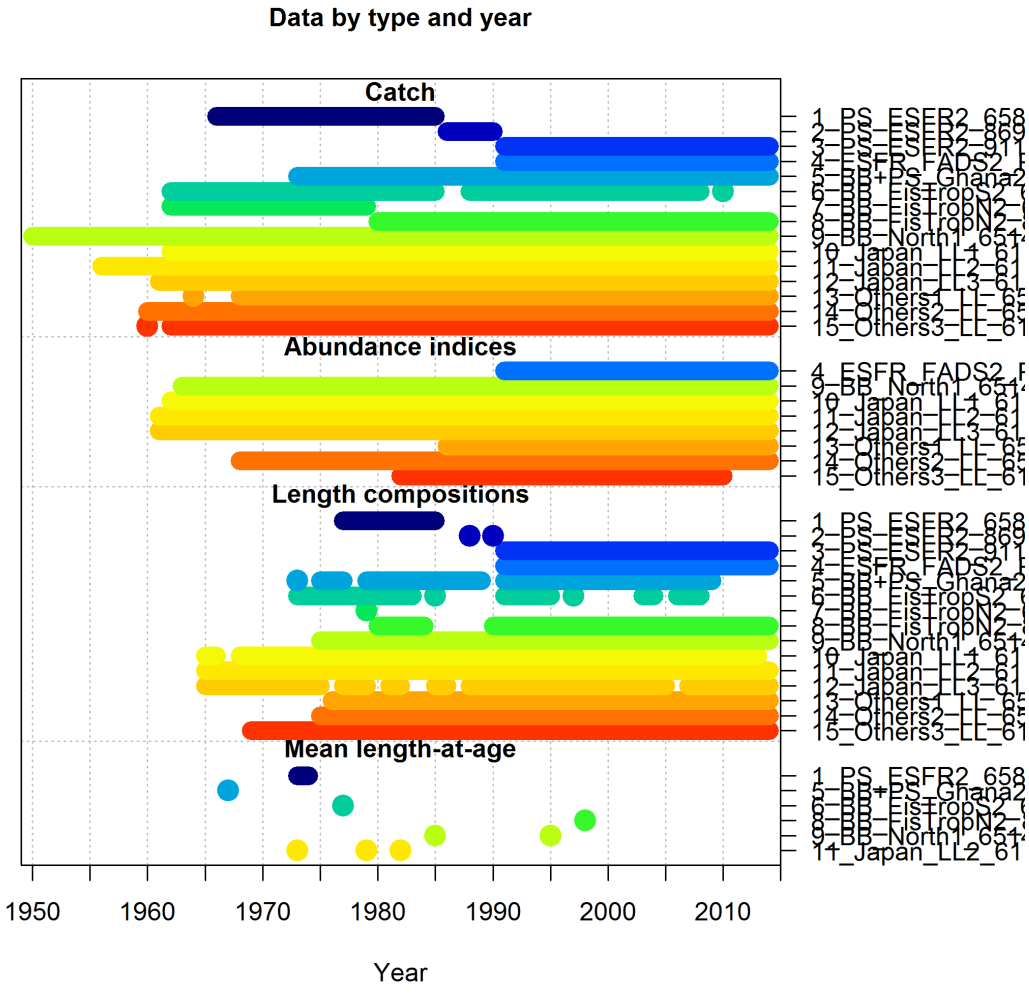

Figure 16. Layout of the BET data available for the 2015 assessment by type, fleet and year/quarter.

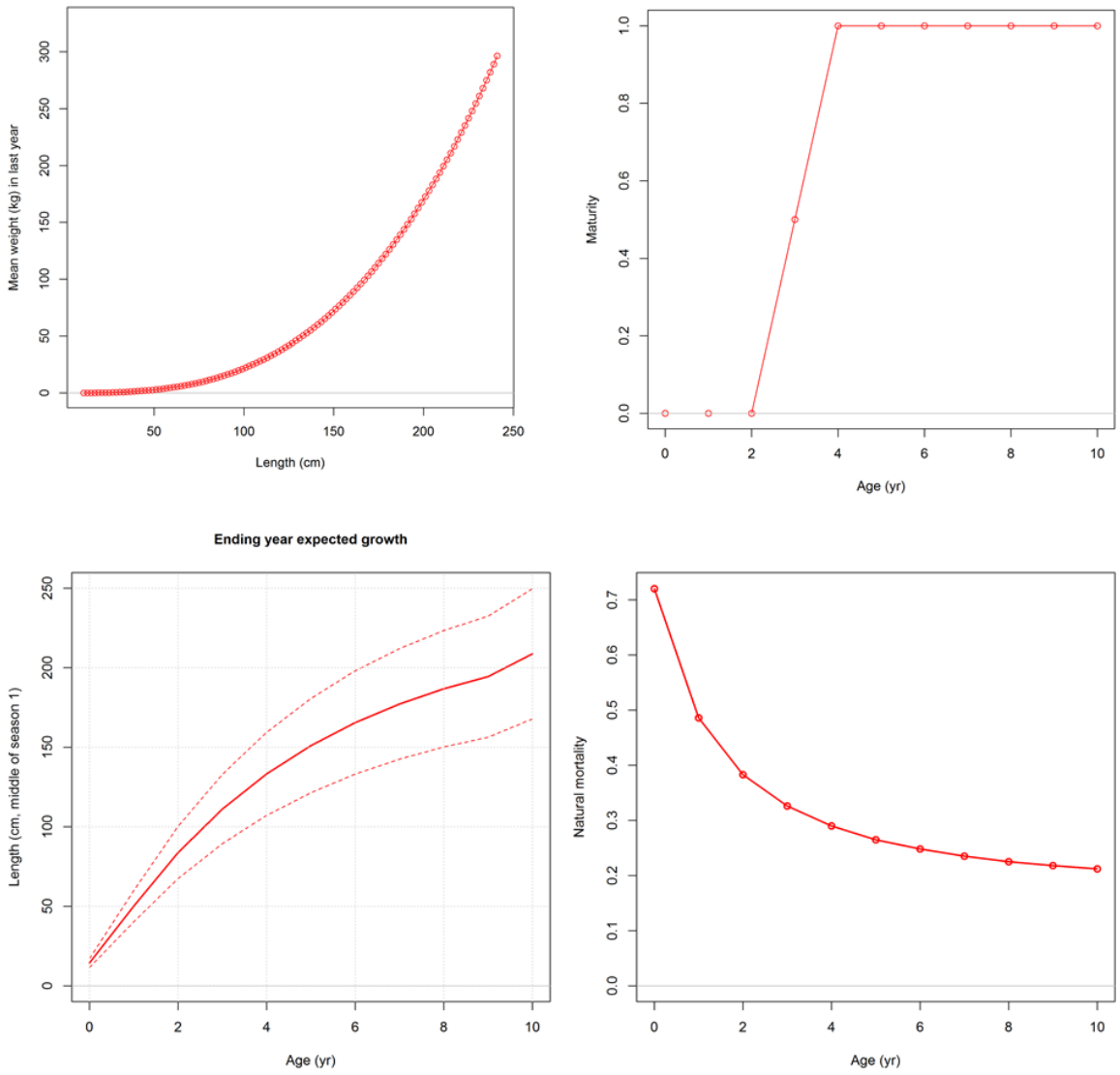

Figure 17 Life history functions used in the BET assessment model: (top left) weight-length, (top right) maturity at age, (bottom left) growth, and (bottom right) natural mortality.

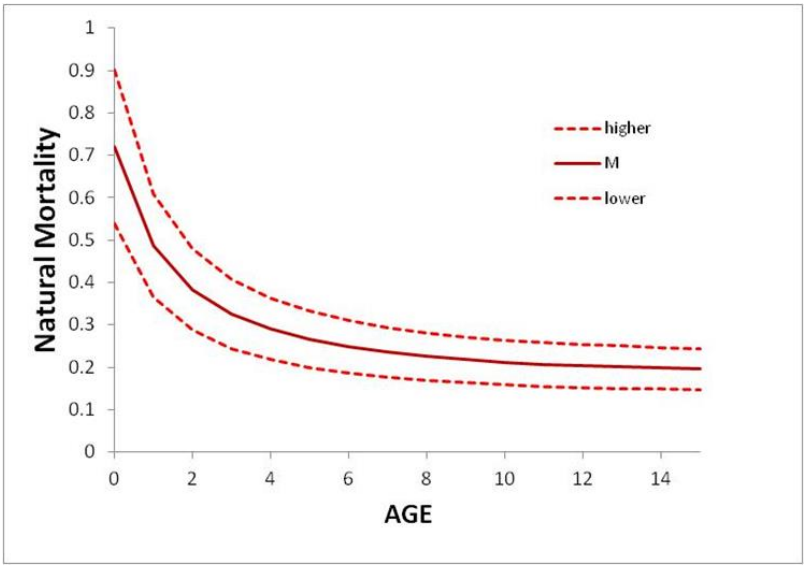

		0.75	M	1.25
Age	Length	Lower	Vector	Upper
0	42	0.540	0.720	0.900
1	71	0.365	0.486	0.608
2	95	0.287	0.383	0.479
3	115	0.245	0.326	0.408
4	132	0.217	0.290	0.362
5	146	0.199	0.265	0.332
6	158	0.186	0.248	0.310
7	168	0.176	0.235	0.294
8	176	0.169	0.225	0.281
9	183	0.163	0.218	0.272
10	188	0.159	0.212	0.265
11	193	0.155	0.207	0.259
12	197	0.152	0.203	0.254
13	200	0.150	0.200	0.250
14	203	0.148	0.198	0.247
15	206	0.147	0.196	0.244

Figure 18. Lorenzen natural mortalities considered and age/length-specific values for bigeye tuna.

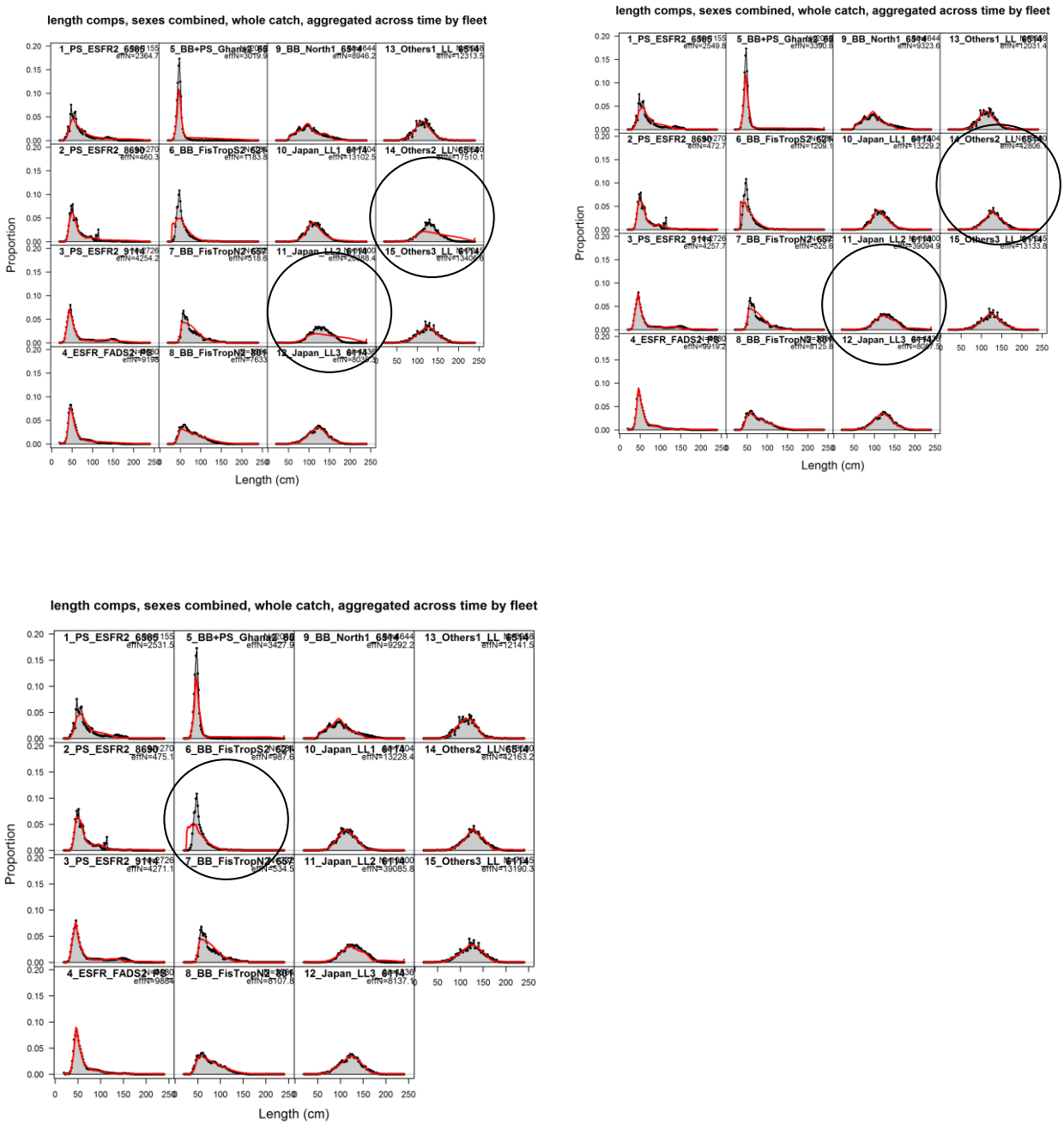

Figure 19. Overall fit to length compositions for (top left) Model_10, (top right) Model_11h, and (bottom) Model_12h.

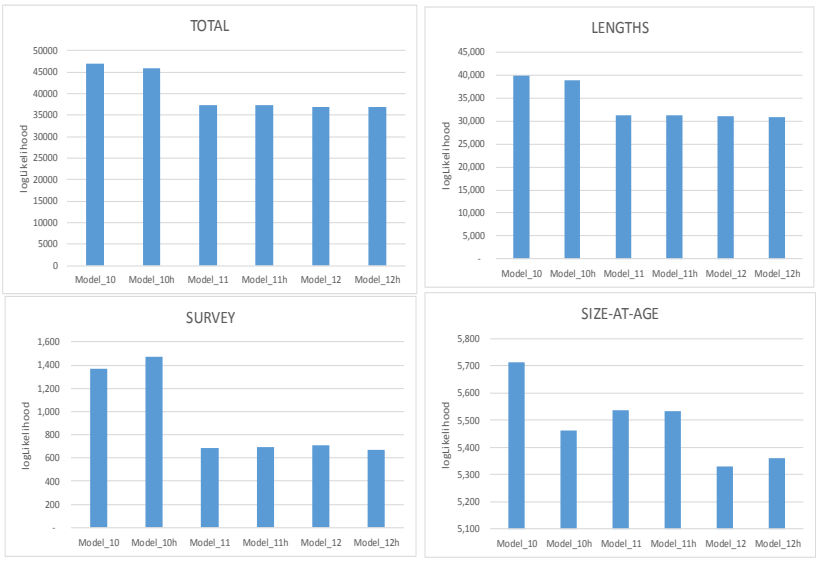

Figure 20. Likelihood values by components for the three candidate models with and without steepness (h) estimated.

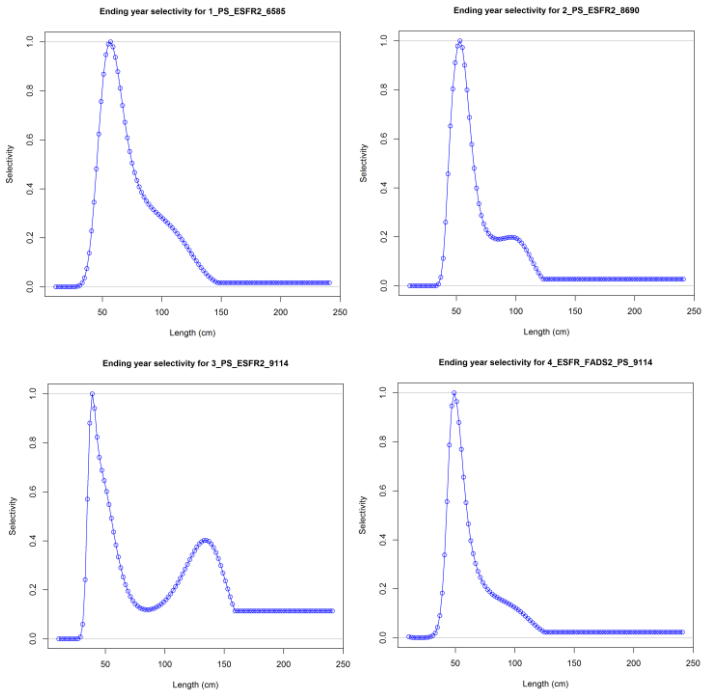

Figure 21. Estimated length-based selectivity for the four purse seine fleets from the base case model.

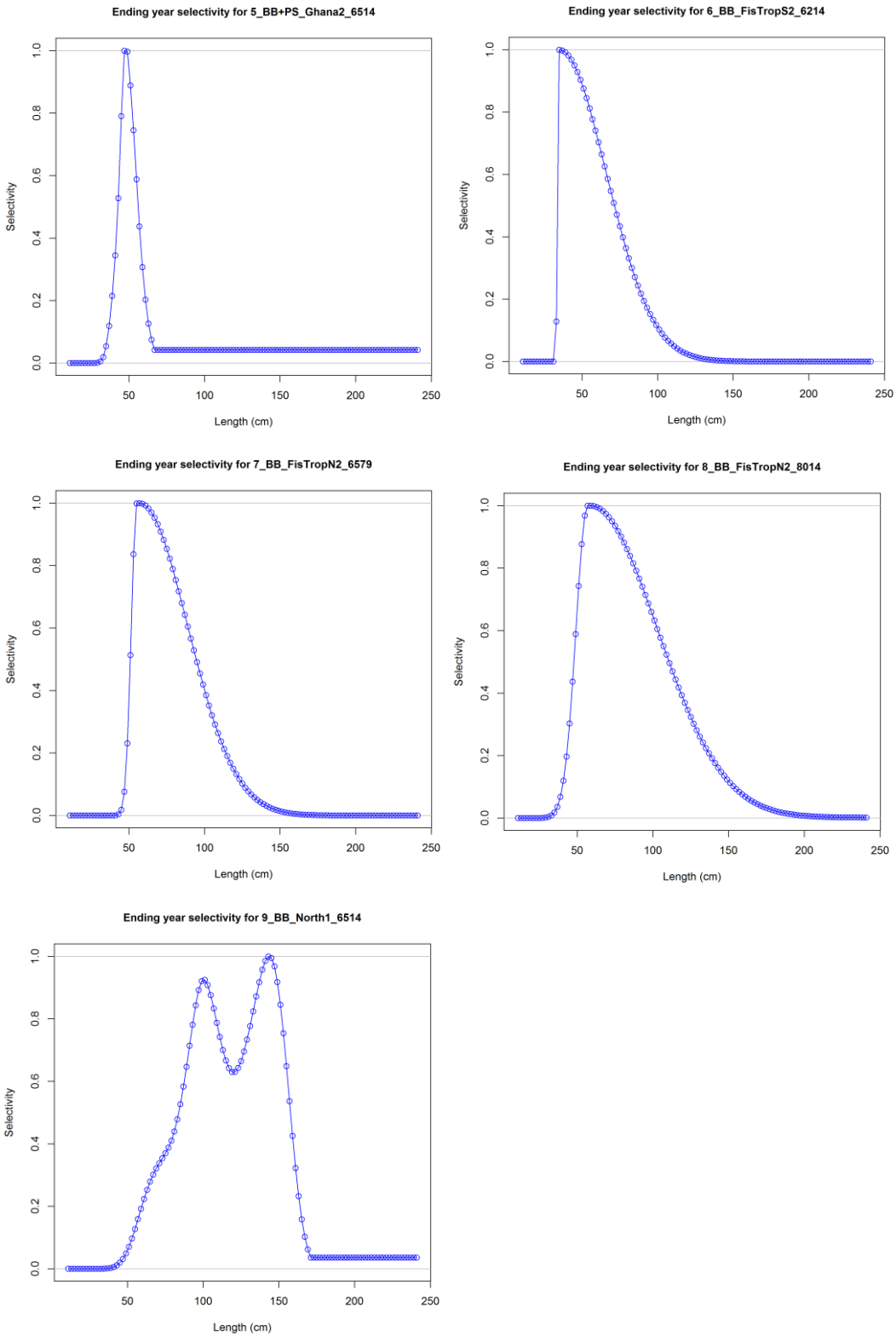

Figure 22. Estimated length-based selectivity for the five baitboat fleets from the base case model.

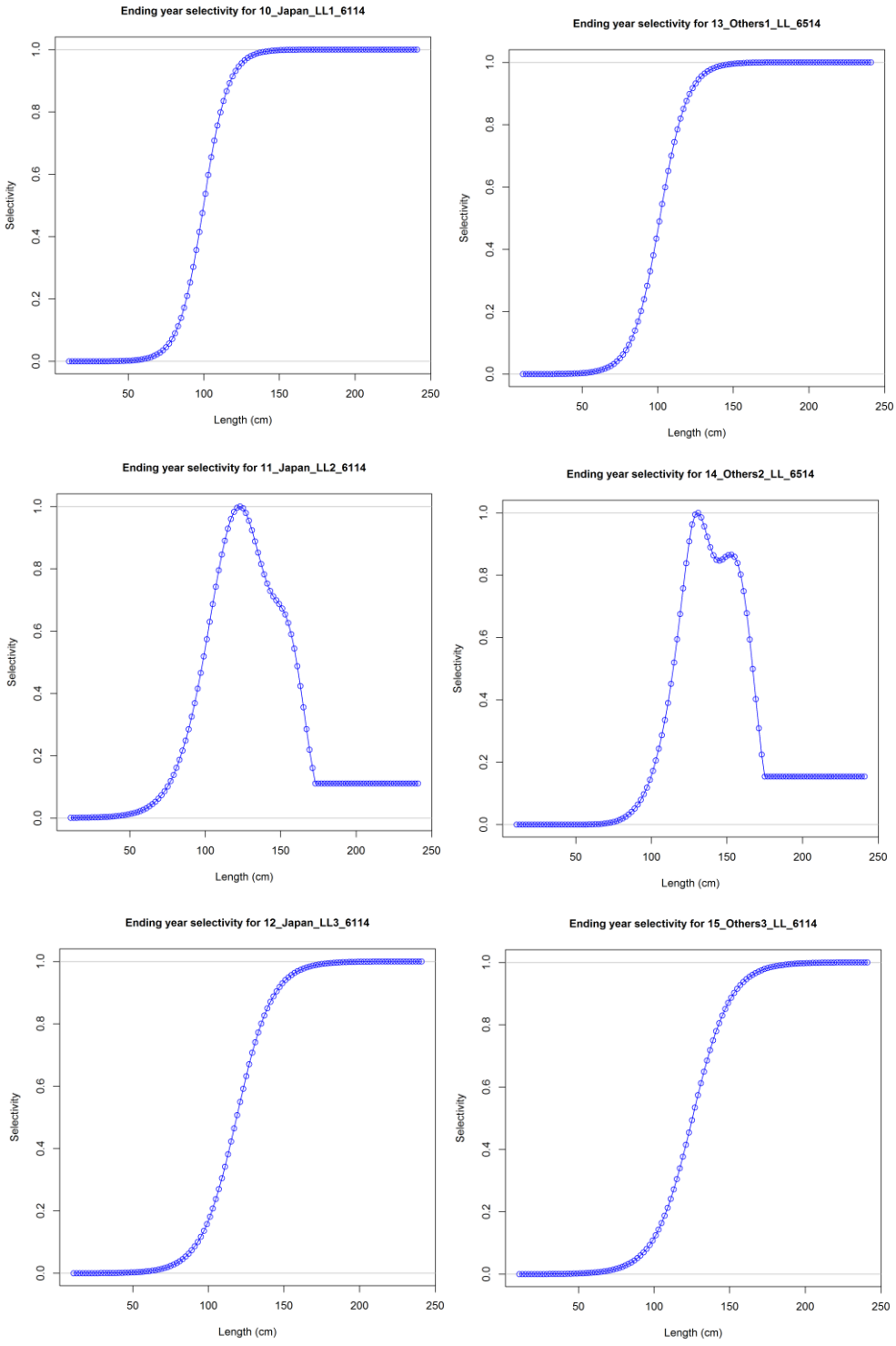

Figure 23. Estimated length-based selectivity for the six longline fleets from the base case model.

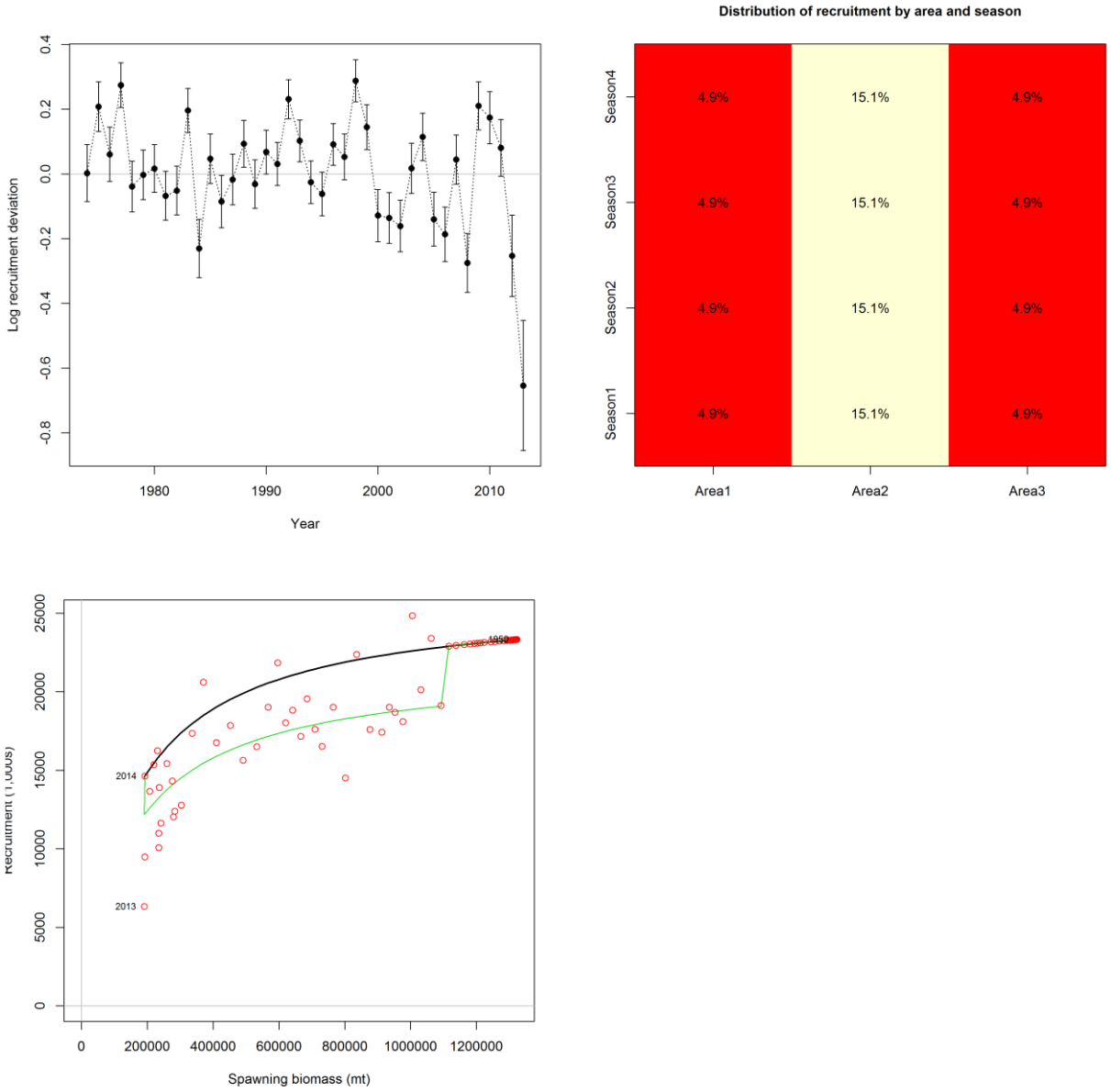

Figure 24. Estimated (top left) annual recruitment deviations, (top right) distribution of recruits within season and area, and (bottom left) stock-recruitment function from the base case model.

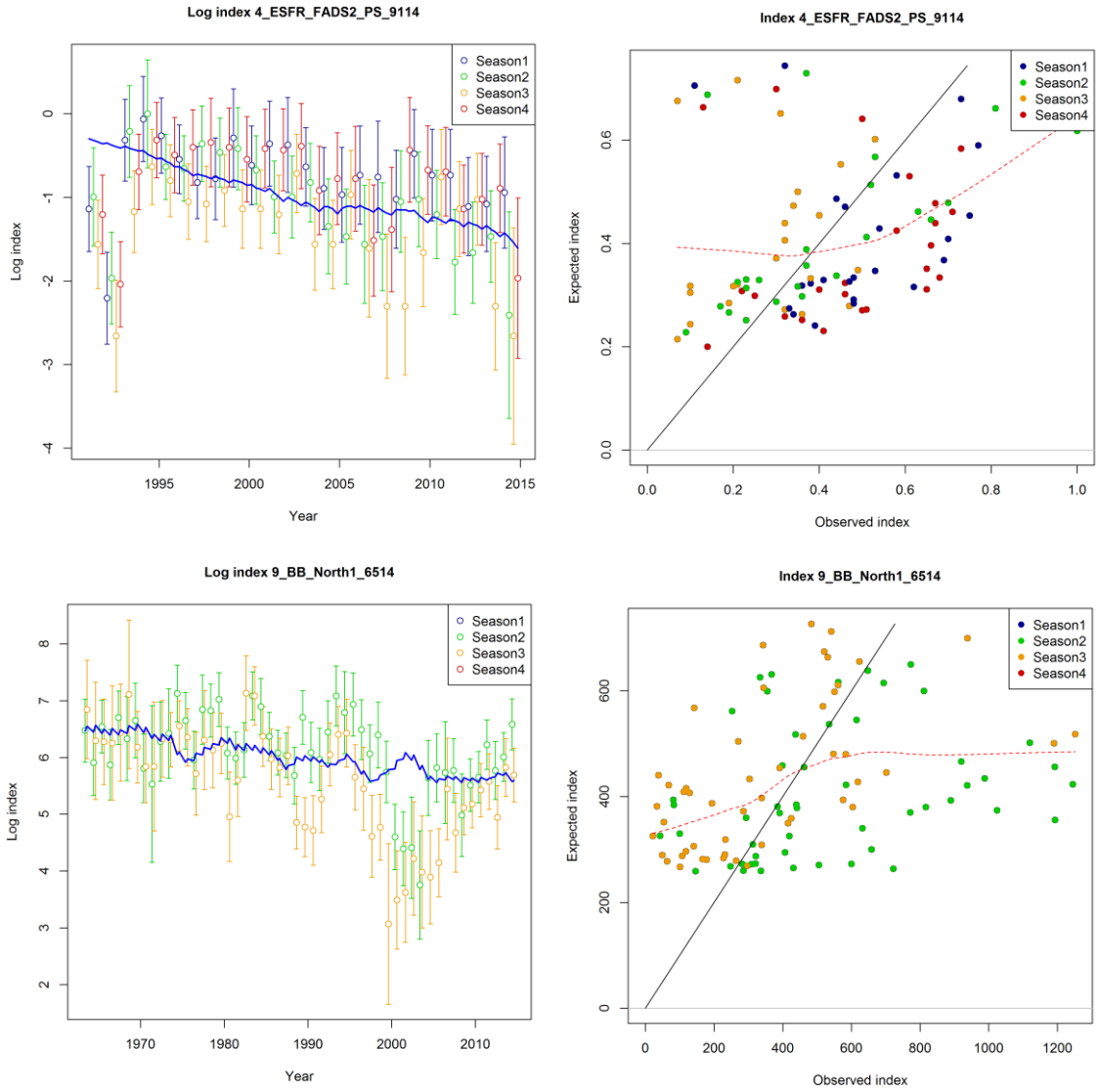

Figure 25. Fit to the CPUE and residuals for the (top) purse seine fishery and (bottom) Azores baitboat fishery.

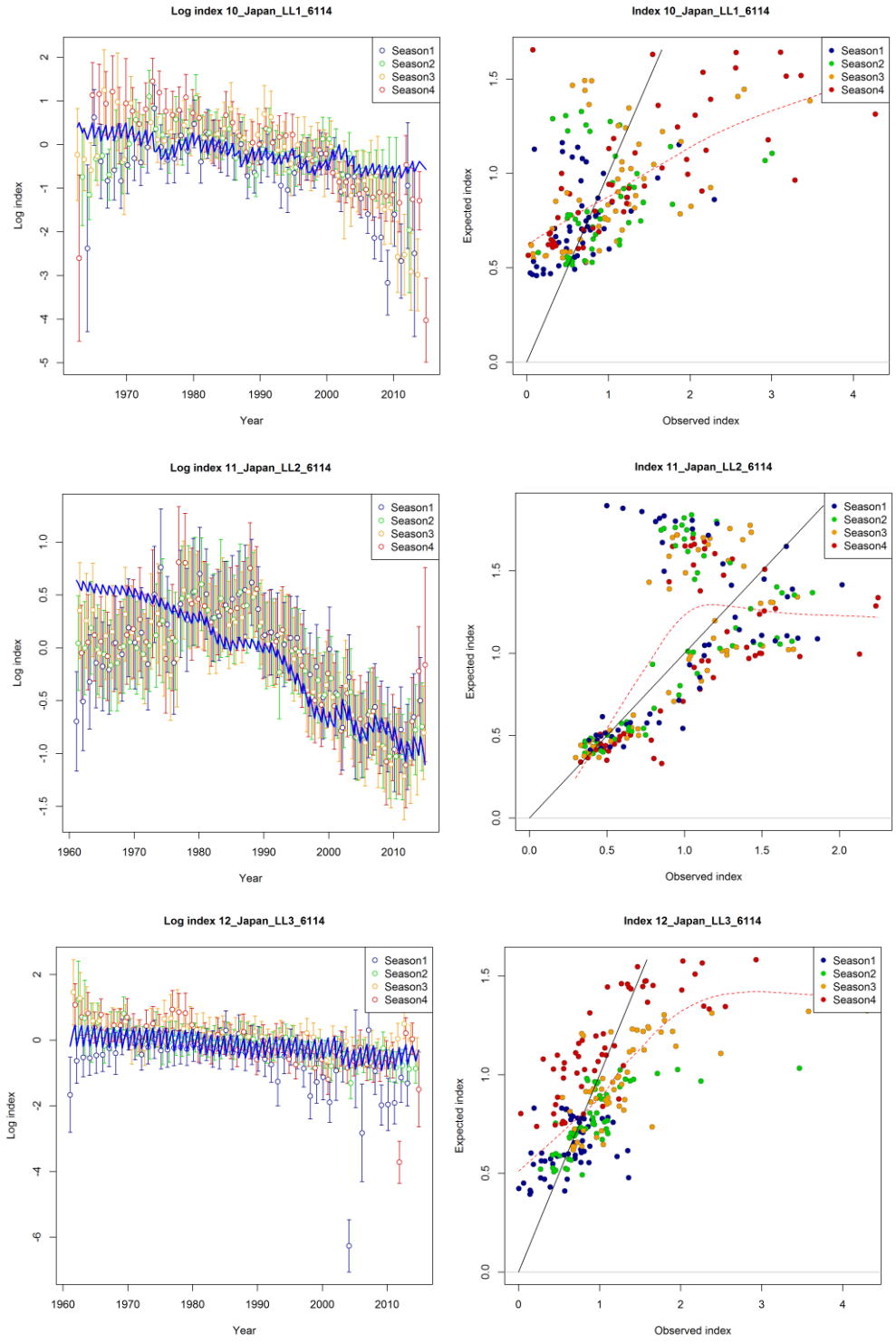

Figure 26. Fit to the CPUE and residuals for the Japanese longline fleets (top) in Area 1, (middle (Area 2), and (bottom) Area 3.

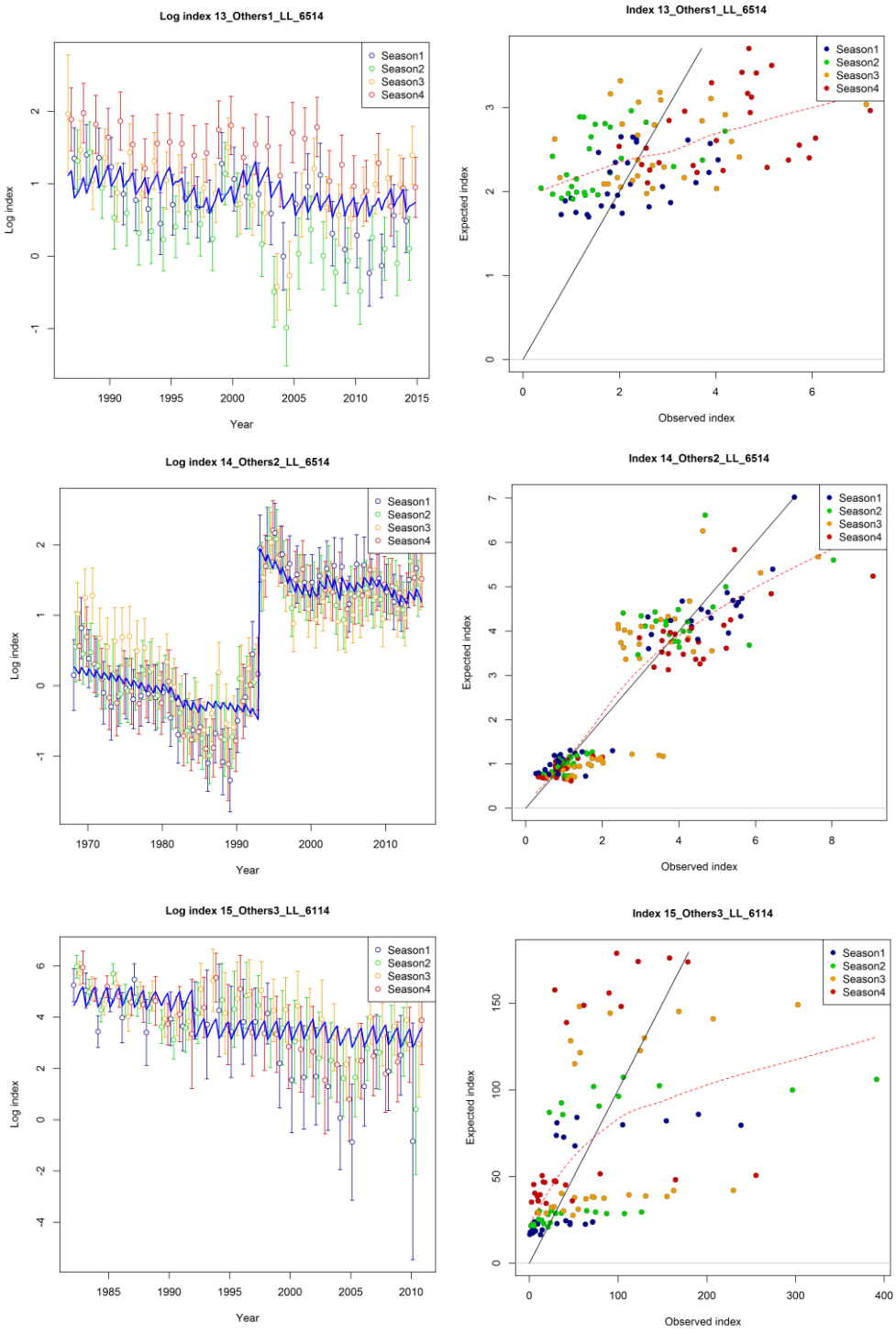

Figure 27. Fit to the CPUE and residuals for the longline fleets (top) US in Area 1, (middle) Chinese-Taipei (Area 2), and Uruguayan (bottom) Area 3.

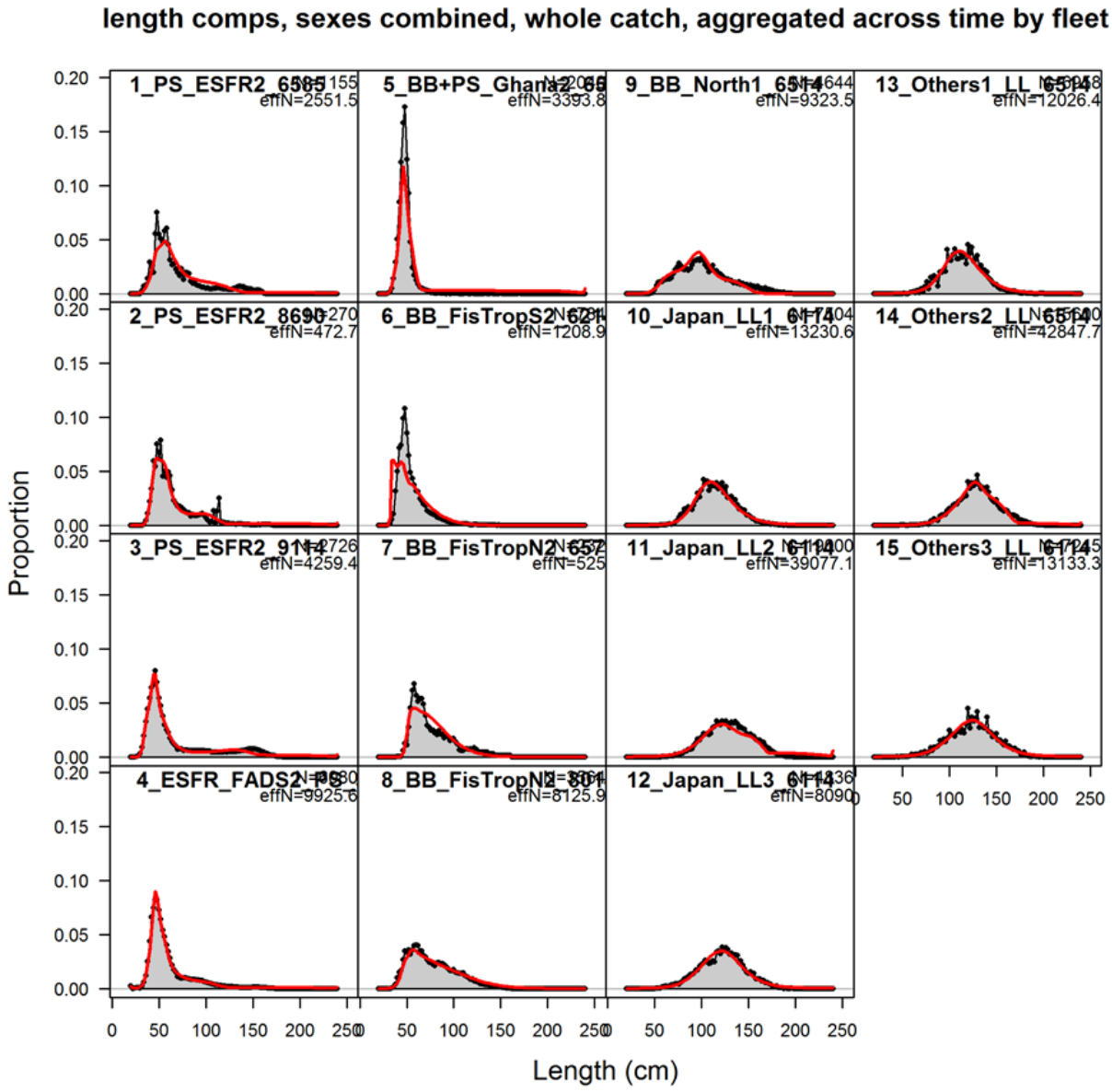

Figure 28. Fit to the length comps aggregated across time by fleet.

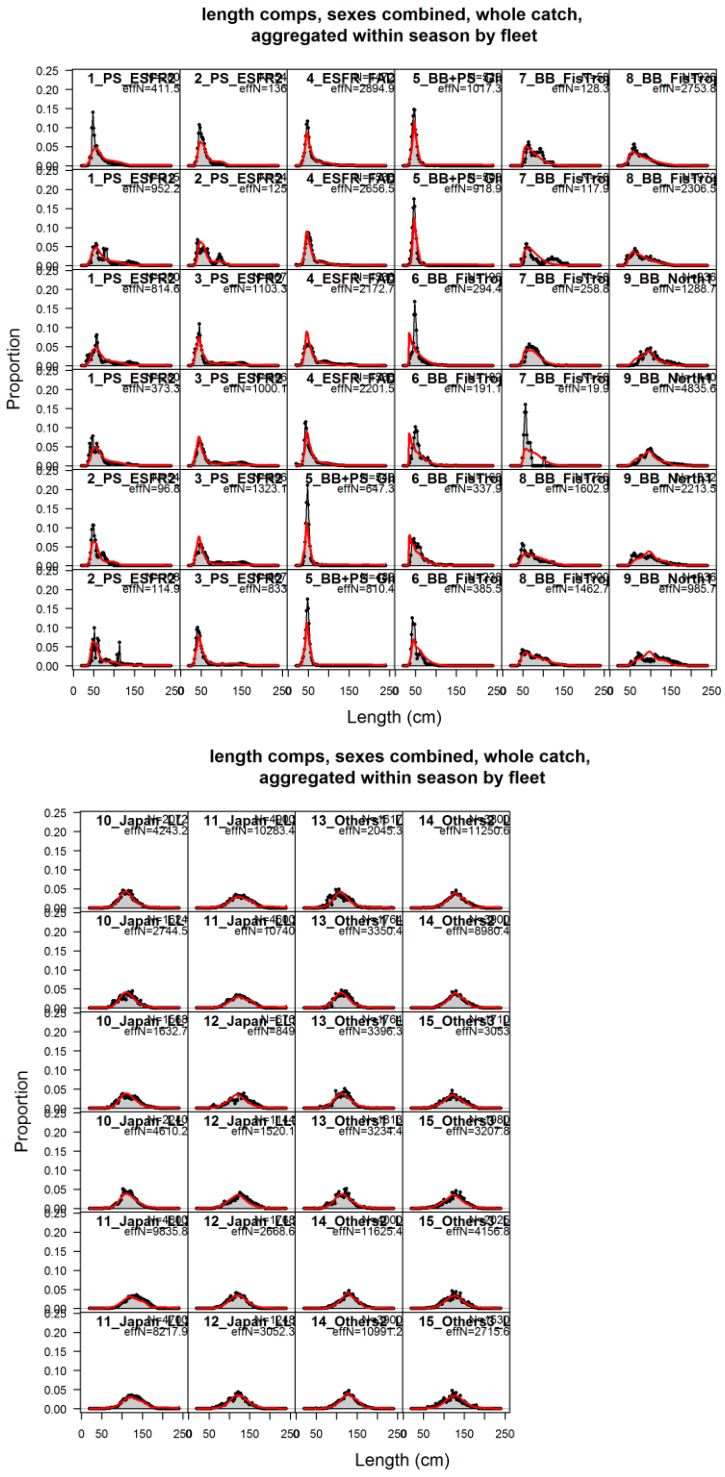

Figure 29. Fit to the length comps aggregated within season by fleet.

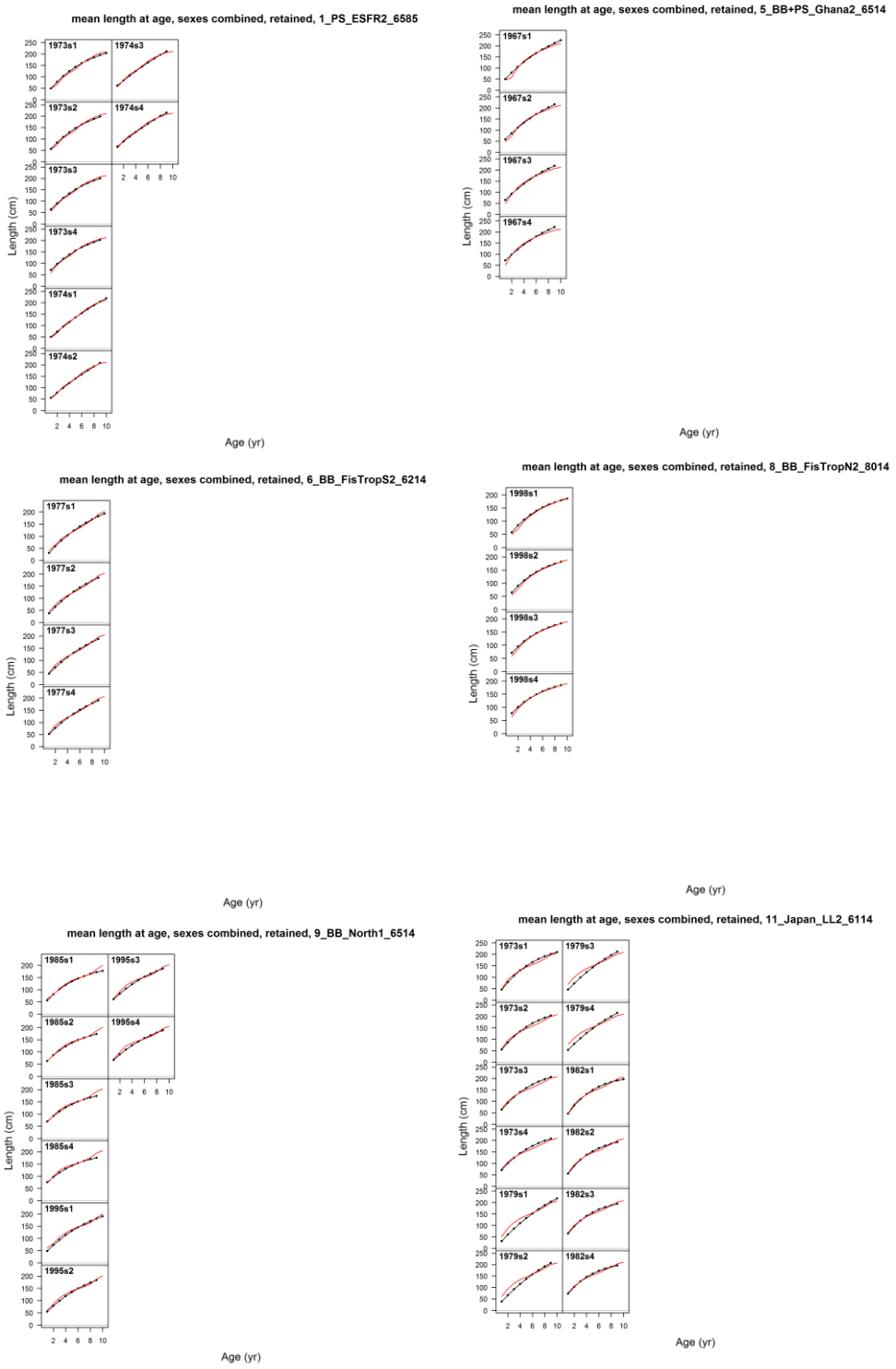

Figure 30. Fit to mean length at age observations by fleet.

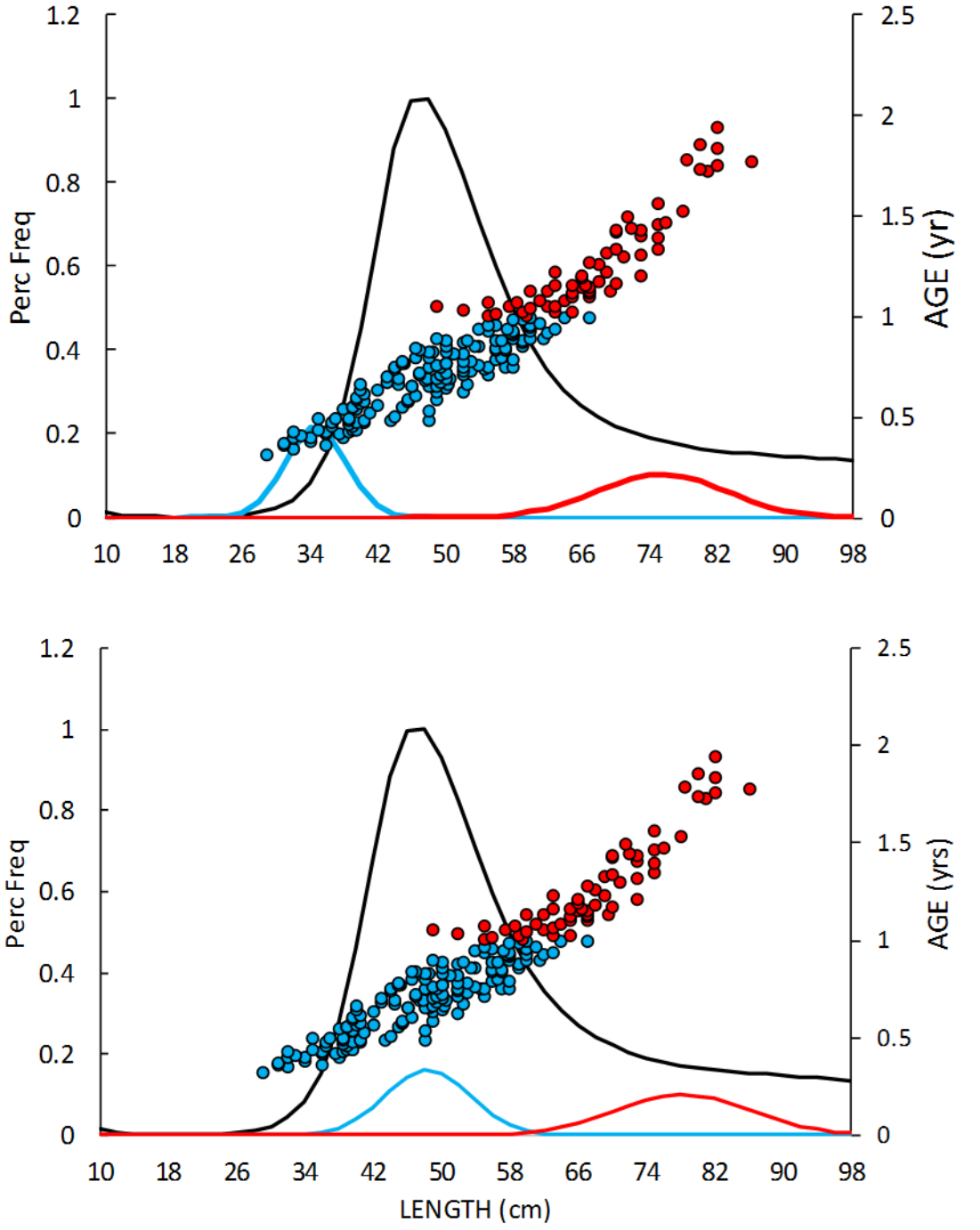

Figure 31. Comparison between (blue dots) observed length at age_0, born in the first quarter and "captured" in the fourth quarter, and (red dots) age_1 fish and the percent frequency of (blue line) age_0 and (red line) age_1 from (top) Model_11h and (bottom) Model_20h. The black line depicts the estimated selectivity of the purse seine FAD fleet (fleet 4).

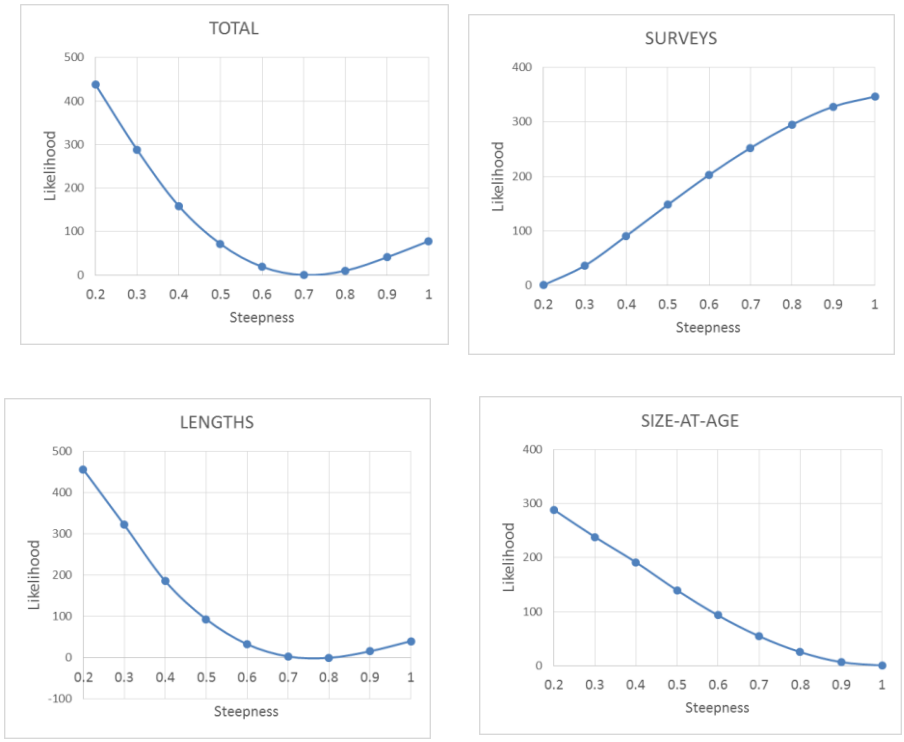

Figure 32. Profile analysis for the steepness parameter for (upper left) Total Likelihood, (top right) CPUE data, (lower left) length compositions, and (lower right) the mean size-at-age data.

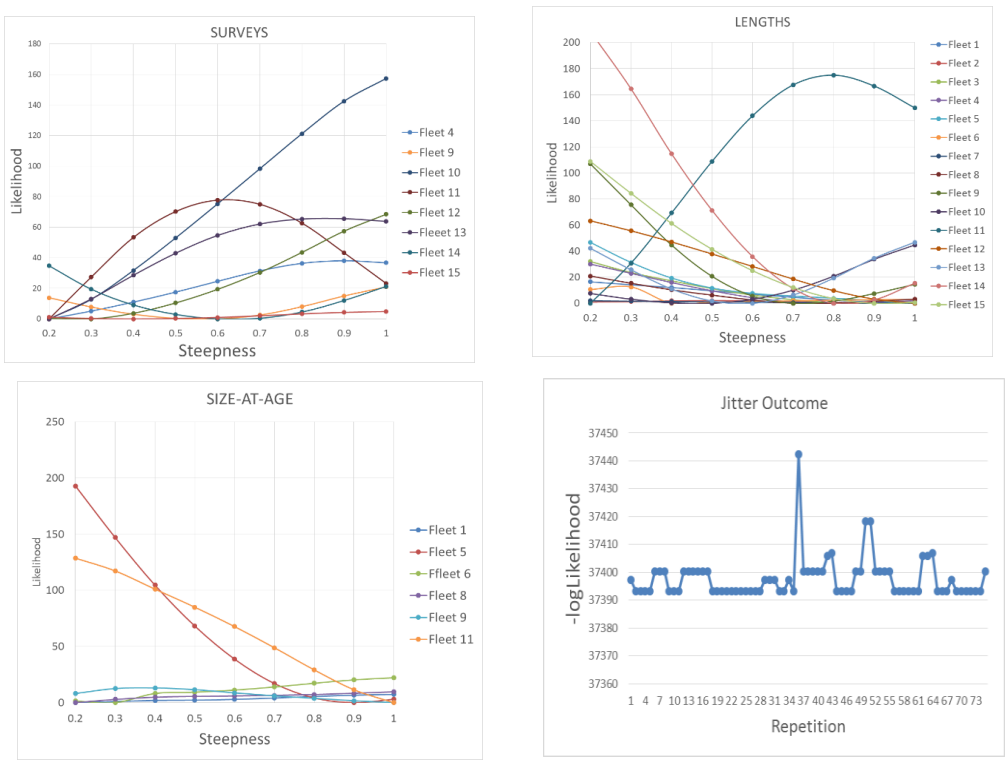

Figure 33. Profile analysis for the steepness parameter for the various fleet specific data sources: (top, left) CPUE's (or surveys), (top, right) length data, and (bottom, left) the mean size-at-age data; (bottom, right) outcome of "jitter" exercise.

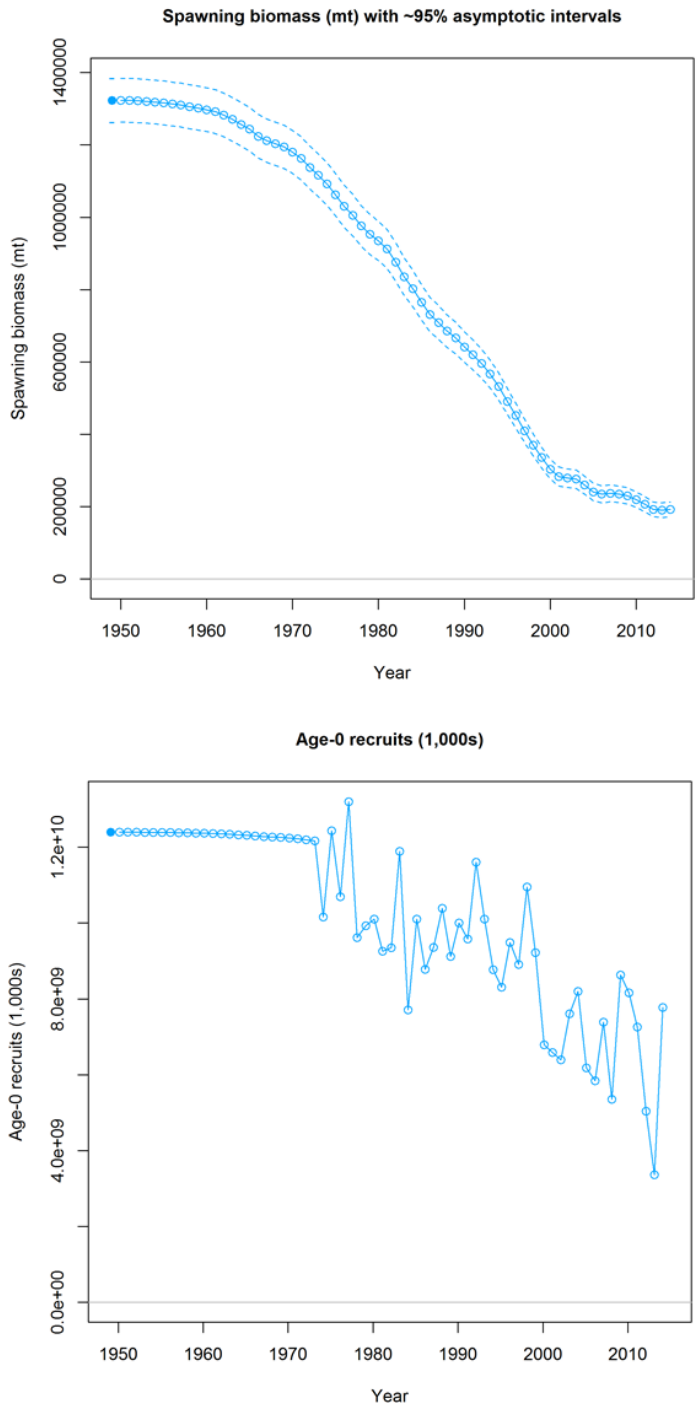

Figure 34. Estimated trends in (top) spawning stock and (bottom) recruitment from the base case model.

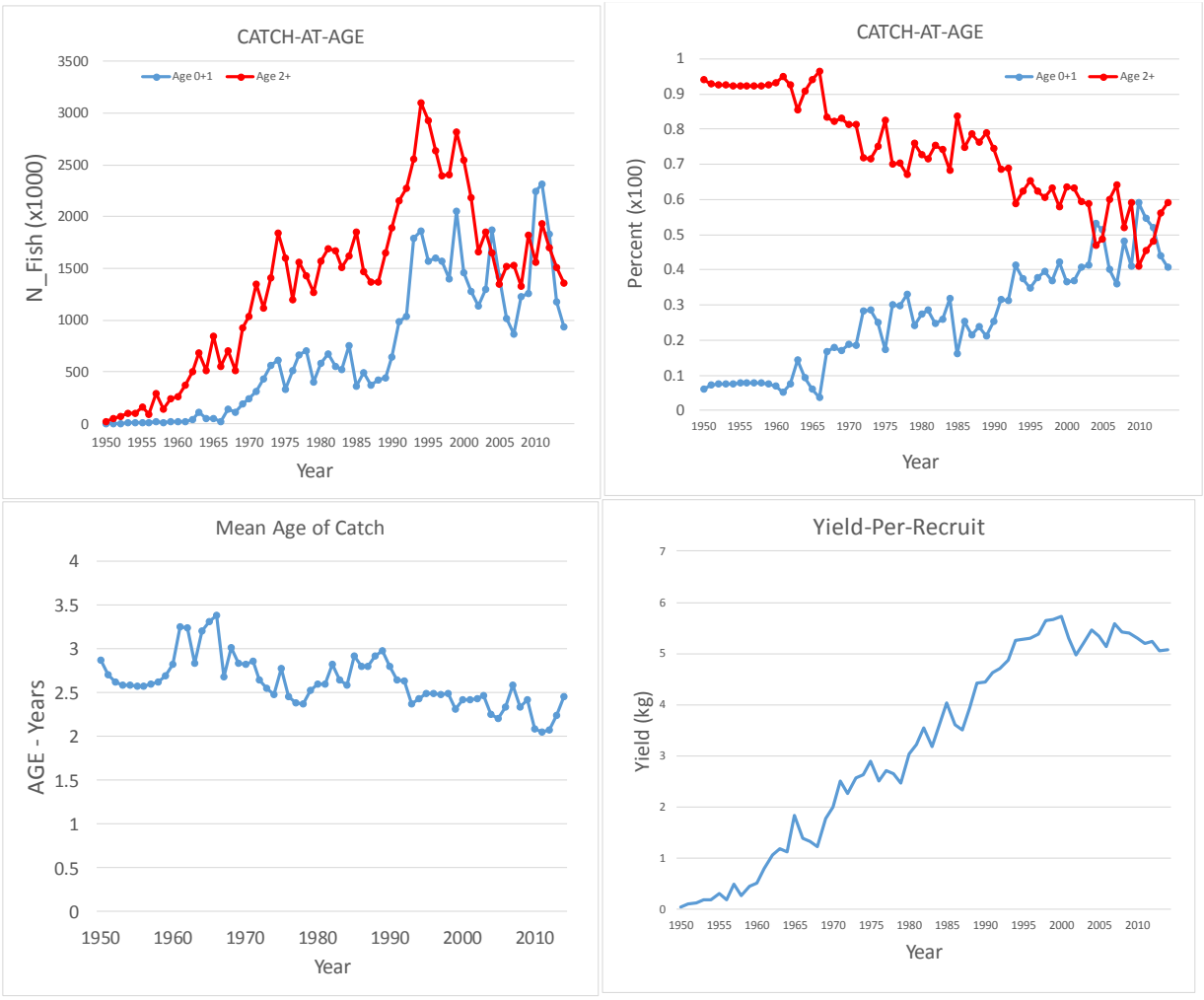

Figure 35. Estimated (top left) catch-at-age broken down into Ages 0+1 and Ages 2+; (top, right) proportion by ages; (bottom left) mean age of catch; and (bottom right) yield-per-recruit.